RM No. E6K26

RESEARCH MEMORANDUM

for the

Air Materiel Command, Army Air Forces

ALTITUDE-WIND-TUNNEL INVESTIGATION OF PERFORMANCE OF SEVERAL PROPELLERS ON YP-47M AIRPLANE AT HIGH BLADE LOADINGS

VI - HAMILTON STANDARD 6507A-2 FOUR- AND THREE-BLADE PROPELLERS

By Martin J. Saari and Solomon M. Sorin

Aircraft Engine Research Laboratory
Cleveland, Ohio

NATIONAL ADVISORY COMMITTEE FOR AERONAUTICS

WASHINGTON

DEC 19 1946

NATIONAL ADVISORY COMMITTEE FOR AERONAUTICS

RESEARCH MEMORANDUM

for the

Air Materiel Command, Army Air Forces

ALTITUDE-WIND-TUNNEL INVESTIGATION OF PERFORMANCE OF SEVERAL PROPELLERS ON YP-47M AIRPLANE AT HIGH BLADE LOADINGS

VI - HAMILTON STANDARD 6507A-2 FOUR- AND THREE-BLADE PROPELLERS

By Martin J. Saari and Solomon M. Sorin

SUMMARY

An altitude-wind-tunnel investigation has been made to determine the performance of Hamilton Standard 6507A-2 four-blade and three-blade propellers on a YP-47M airplane at high blade loadings and high engine powers. Characteristics of the four-blade propeller were obtained for a range of power coefficients from 0.10 to 1.00 at free-stream Mach numbers of 0.20, 0.30, and 0.40. Characteristics of the three-blade propeller were obtained for a range of power coefficients from 0.30 to 1.00 at a free-stream Mach number of 0.40. Results of the force measurements indicate primarily the trend of propeller efficiency for changes in power coefficient or advance-diameter ratio because no corrections for the effects of tunnel-wall constriction on the installation were applied. Slipstream surveys are presented to illustrate blade thrust load distribution for certain operating conditions.

Within the range of advance-diameter ratios investigated at each free-stream Mach number, the efficiency of the four-blade propeller decreased as the power coefficient was increased from 0.10 to 1.00. For the three-blade propeller, nearly constant maximum efficiencies were obtained for power coefficients from 0.32 to 0.63 at advance-diameter ratios between 1.90 and 3.00.

In general, for conditions below the stall and critical tip Mach number, the maximum thrust load shifted from the inboard sections toward the tip sections as the power coefficient was increased or as the advance-diameter ratio was decreased. For conditions beyond the

stall or critical tip Mach number, losses in thrust occurred on the outboard blade sections owing to flow break-down; the thrust load increased slightly on the inboard sections.

INTRODUCTION

An investigation of the performance of several propellers on a YP-47M airplane at high blade loadings has been made in the Cleveland altitude wind tunnel at the request of the Air Materiel Command, Army Air Forces. As part of the program, Hamilton Standard 6507A-2 four-blade and three-blade propellers were investigated.

Characteristics of the four-blade propeller were obtained for a range of power coefficients from 0.10 to 1.00 at free-stream Mach numbers of 0.20, 0.30, and 0.40. Characteristics of the three-blade propeller were obtained for a range of power coefficients from 0.30 to 1.00 at a free-stream Mach number of 0.40.

As in references 1 to 5, propeller efficiencies were determined from force measurements and the blade thrust load distribution was obtained with two diametrically opposed slipstream survey rakes.

PROPELLER AND POWER PLANT

The propellers and power plant are described as follows:

Propeller	
Blade design	Hamilton Standard 6507A-2
Blade sections	NACA 16 series
Propeller diameter, four-blade	13 feet 0 inch
Propeller diameter, three-blade	12 feet 10 inches
Activity factor[1]	104
Propeller gear ratio	20:9
Engine	R-2800-73
War emergency power rating:	
Engine speed, rpm	2800
Manifold pressure, in. Hg	72.0
Brake horsepower	2800
Military power rating:	
Engine speed, rpm	2800
Manifold pressure, in. Hg	53.5
Brake horsepower	2100

Normal power rating:	
Engine speed, rpm	2600
Manifold pressure, in. Hg	41.5
Brake horsepower	1700

[1]The activity factor is a nondimensional function of the propeller plan form designed to express the integrated capacity of the blade elements for absorbing power. (See reference 1.)

The propeller blade-form characteristics are given in figure 1. A photograph of the Hamilton Standard 6507A-2 propeller blade is shown in figure 2.

APPARATUS AND PROCEDURE

The four-blade and three-blade propellers installed on the YP-47M airplane in the 20-foot-diameter test section of the altitude wind tunnel are shown in figures 3 and 4, respectively. A description of the equipment is given in reference 1.

The characteristics of the four-blade propeller were obtained for a range of power coefficients from 0.10 to 1.00 at free-stream Mach numbers of 0.20, 0.30, and 0.40. The investigation was conducted at density altitudes from 5000 to 45,000 feet, engine powers from 150 to 2700 brake horsepower, and engine speeds from 1400 to 3000 rpm.

The characteristics of the three-blade propeller were obtained for a range of power coefficients from 0.30 to 1.00 at a free-stream Mach number of 0.40. Density altitudes ranged from 20,000 to 40,000 feet, engine powers from 300 to 1850 brake horsepower, and engine speeds from 1200 to 2900 rpm.

REDUCTION OF DATA

The method of data reduction was the same as that given in reference 1. The analysis of the force measurements was made in terms of the variation of propeller efficiency η with the propeller power coefficient C_P and the advance-diameter ratio J. These parameters were determined by the following equations:

$$C_P = \frac{P}{\rho n^3 D^5}$$

where

D propeller diameter, feet

n propeller rotational speed, revolutions per second

P engine power, foot-pounds per second

ρ free-stream density, slugs per cubic foot

$$J = \frac{V}{ND}$$

where V is the free-stream velocity in feet per second.

$$\eta = \frac{C_T J}{C_P}$$

The propeller thrust coefficient C_T in the efficienty formula is defined as

$$C_T = \frac{T}{\rho n^2 D^4}$$

where T is the propeller thrust in pounds.

The propeller tip Mach number was obtained from the relation

$$M_t = M_O \sqrt{1 + \left(\frac{\pi}{J}\right)^2}$$

where M_O is the free-stream Mach number.

The slipstream surveys were presented as plots of the total-pressure rise $H_s - H_O$ across the propeller disk against the square of the radius ratio $(r_s/R)^2$

where

H_O free-stream total pressure, pounds per square foot

H_s total pressure at survey point, pounds per square foot

R propeller radius to tip, inches

r_s radial distance from thrust axis to survey point, inches

RESULTS AND DISCUSSION

The performance of the four-blade propeller at various blade loading conditions is presented separately for free-stream Mach numbers of 0.20, 0.30, and 0.40 because it is impossible to compare the data obtained at different free-stream Mach numbers inasmuch as tunnel-wall constriction effects vary with airspeed. Characteristics of the three-blade propeller were determined only at a free-stream Mach number of 0.40. As in references 1 to 5, the results of the force measurements are of value primarily in showing the trend of propeller efficiency for changes in power coefficient or advance-diameter ratio. The force measurements of the four-blade and three-blade propellers are not comparable inasmuch as the propeller efficiencies were calculated by means of an average installation drag coefficient. (See reference 1.) Slipstream surveys are presented to illustrate blade thrust load distribution for certain operating conditions.

Four-Blade Propeller

Free-stream Mach number, 0.20. - The characteristics of the four-blade propeller are presented in figure 5 for a range of power coefficients from 0.10 to 0.90 at a free-stream Mach number of 0.20.

For the range of advance-diameter ratios investigated the propeller efficiency decreased rapidly with an increase in power coefficient or decrease in advance-diameter ratio. The low values of efficiency and the large slope of the efficiency curves indicate that the propeller blades were operating beyond the stall or critical tip Mach number for most of the conditions above a power coefficient of 0.20.

Slipstream surveys showing the effect of power coefficient on blade thrust load distribution are presented in figures 6 and 7 for advance-diameter ratios of approximately 1.00 and 1.30, respectively. At an advance-diameter ratio of 1.00 and a power coefficient of 0.50 (fig. 6(a)), blade stall occurred on sections outboard of $(r_s/R)^2 = 0.40$. The losses in thrust loading on the outboard sections became larger as the power coefficient was increased from 0.50 to 0.70 at an approximately constant advance-diameter ratio (figs. 6(b) and 6(c)). At an advance-diameter ratio of about 1.30, the blade thrust load distribution for a power coefficient of 0.47 was fairly uniform (fig. 7(a)). An increase in power coefficient to 0.58 resulted in flow break-down on sections outboard of $(r_s/R)^2 = 0.40$

and a further increase in power coefficient to 0.67 caused larger losses in thrust on the outboard sections (figs. 7(b) and 7(c)).

No comparison of the magnitudes of the thrust loadings in this report is valid, unless otherwise stated, because the surveys were obtained over a wide range of density altitudes. The difference between the right and left surveys was due to a slight misalinement of the approaching airstream and propeller thrust axis. (See reference 6.)

The effect of advance-diameter ratio on blade thrust load distribution is shown by the slipstream surveys in figures 8 to 10 for power coefficients of approximately 0.20, 0.40, and 0.80. The maximum thrust load shifted toward the tip sections as the advance-diameter ratio was decreased from 1.13 to 0.62 for a power coefficient of 0.20. The survey for an advance-diameter ratio of 0.62 (fig. 8(c)) does not show any serious compressibility losses although the tip Mach number was about 0.93. At a power coefficient of about 0.40 (fig. 9), the blade thrust load distribution for an advance-diameter ratio of 1.05 was uniform, but a decrease in advance-diameter ratio to 0.81 resulted in serious flow break-down on the outboard sections causing the load to shift inboard. At a power coefficient of about 0.80 and an advance-diameter ratio of 1.55 (fig. 10), the outboard blade sections were stalled and a reduction in advance-diameter ratio to 0.99 had no radical effect on the blade thrust load distribution.

Free-stream Mach number, 0.30. - The characteristics of the four-blade propeller are presented in figure 11 for a range of power coefficients from 0.10 to 1.00 at a free-stream Mach number of 0.30.

Within the range of advance-diameter ratios investigated, the highest efficiencies were obtained at power coefficients from 0.10 to 0.40. The propeller efficiency decreased with an increase in power coefficient. The propeller blades were apparently stalled or the critical tip Mach number had been exceeded for most conditions above a power coefficient of 0.50 (fig. 11).

The effect of power coefficient on blade thrust load distribution is shown in figure 12 for the conditions of figure 11 at an advance-diameter ratio of about 1.30. At a power coefficient of 0.09 the maximum thrust loading occurred on the inboard sections and a change in power coefficient to 0.19 shifted the maximum thrust load toward the tip sections (figs. 12(a) and 12(b)). At a power coefficient of 0.50, flow break-down occurred on the outboard sections caused by a combination of stall and compressibility effects (fig. 12(c)).

The effect of advance-diameter ratio on blade thrust load distribution is shown in figures 13, 14, and 15 for power coefficients of approximately 0.20, 0.40, and 0.50, respectively. In general, the slipstream surveys for each of the power coefficients indicate that, for conditions below the stall or critical tip Mach number, the maximum thrust load shifted toward the tip sections as the advance-diameter ratio was decreased. Serious flow break-down at the outboard section was evident at a power coefficient of 0.50 and an advance-diameter ratio of 1.21 (fig. 15(c)).

Free-stream Mach number, 0.40. - The variation of the efficiency of the four-blade propeller with advance-diameter ratio is presented in figure 16 for power coefficients from 0.10 to 1.00 at a free-stream Mach number of 0.40.

The range of advance-diameter ratios investigated was below the value for peak efficiencies for all power coefficients above 0.10. In this range of advance-diameter ratios the propeller efficiency decreased rapidly as the power coefficient was increased above 0.10.

The effect of power coefficient on blade thrust load distribution is shown by the slipstream surveys in figure 17, which correspond to the conditions of figure 16 at an advance-diameter ratio of approximately 2.10. At a power coefficient of 0.09 (fig. 17(a)) the thrust loading was low and the loading on the inboard sections was slightly greater than on the tip sections. As the power coefficient was increased from 0.09 to 0.61 (figs. 17(b) to 17(d)), the over-all thrust load increased and the maximum load shifted toward the tip sections. Flow break-down occurred on the outboard sections at a power coefficient of 0.99 (fig. 17(e)).

Three-Blade Propeller

Free-stream Mach number, 0.40. - Performance characteristics of the three-blade propeller are shown in figure 18 for a range of power coefficients from 0.32 to 1.00 at a free-stream Mach number of 0.40.

Nearly constant maximum efficiencies were obtained for power coefficients from 0.32 to 0.63 for advance-diameter ratios between 1.90 and 3.00. As the power coefficient was increased the peak efficiency occurred at generally increasing advance-diameter ratios. The propeller efficiency for the high power coefficients decreased rapidly as the advance-diameter ratio was reduced below 2.80 (fig. 18).

The effect of power coefficient on blade thrust load distribution is shown by the slipstream surveys in figures 19, 20, and 21, which correspond to the conditions of figure 18 for advance-diameter ratios of approximately 1.75, 2.10, and 2.90, respectively. At an advance-diameter ratio of 1.78 and a power coefficient of 0.32 (fig. 19(a)) the thrust load on the outboard sections was somewhat greater than on the inboard sections. A change in power coefficient to 0.53 at nearly the same advance-diameter ratio (fig. 19(b)) resulted in flow break-down on the outboard sections. The loss in thrust due to flow break-down increased considerably as the power coefficient was further increased to 0.65 (fig. 19(c)).

At an advance-diameter ratio of approximately 2.10, the blade thrust load distributions for power coefficients 0.39 and 0.53 were uniform and similar except that, as the power coefficient was increased, the maximum load shifted slightly toward the tip sections (figs. 20(a) and 20(b)). The right survey for a power coefficient of 0.63 (fig. 20(c)) indicates initial stall on the outboard sections. At power coefficients from 0.74 to 1.07 (figs. 20(d) to 20(g)) serious flow break-down occurred on the outboard sections and the thrust load increased slightly on the inboard sections.

At an advance-diameter ratio of about 2.87 the blade thrust loading was uniform for a power coefficient of 0.62 (fig. 21(a)). The thrust load distribution for power coefficients of 0.75 and 0.85 (figs. 21(b) and 21(c)) were also fairly uniform except that the right surveys dip slightly at the outboard sections, indicating initial blade stall. At a power coefficient of 1.03 (fig. 21(d)) flow break-down occurred on sections outboard of $(r_s/R)^2 = 0.35$.

The effect of advance-diameter ratio on blade thrust load distribution is shown in figures 22, 23, and 24 for power coefficients of 0.32, 0.53, and 0.63, respectively. At a power coefficient of 0.32, the thrust loading increased and the maximum load shifted gradually from the inboard sections to the outboard sections as the advance-diameter ratio was reduced from 3.06 to 1.78 (figs. 22(a) to 22(d)). A further reduction in advance-diameter ratio to 1.44, which corresponds to a tip Mach number of 0.97, resulted in compressibility losses on sections outboard of $(r_s/R)^2 = 0.60$ (fig. 22(e)).

At a power coefficient of 0.53 the thrust load distribution for advance-diameter ratios from 3.32 to 2.19 (figs. 23(a) to 23(c)) were uniform and similar except that the maximum load shifted slightly toward the tip sections as the advance-diameter ratio was reduced. Stall and compressibility effects became evident at an advance-diameter ratio of 1.72 (fig. 23(d)).

At a power coefficient of about 0.63 the thrust load distribution for advance-diameter ratios of 3.60 and 2.87 (figs. 24(a) and 24(b)) were uniform and similar. Initial blade stall was apparent at an advance-diameter ratio of 2.15 (fig. 24(c)) and a decrease in advance-diameter ratio to 1.78 (fig. 24(d)) caused serious flow break-down on sections outboard of $(r_s/R)^2 = 0.40$.

SUMMARY OF RESULTS

The results of the force measurements are indicative only of the trend in propeller efficiency with changes in power coefficient or advance-diameter ratio inasmuch as no corrections for the effects of tunnel-wall constriction on the installation were applied.

The investigation in the altitude wind tunnel of Hamilton Standard 6507A-2 four-blade and three-blade propellers on the YP-47M airplane indicated that:

1. Within the range of advance-diameter ratios investigated at each of the free-stream Mach numbers, the efficiency of the four-blade propeller decreases as the power coefficient was increased from 0.10 to 1.00.

2. For the three-blade propeller, nearly constant maximum efficiencies were obtained for power coefficients from 0.32 to 0.63 at advance-diameter ratios between 1.90 and 3.00.

3. In general, for conditions below the stall or critical tip Mach number, the maximum blade thrust loading shifted from the inboard sections toward the tip sections as the power coefficient was increased or as the advance-diameter ratio was decreased.

For conditions beyond the stall or critical tip Mach number, losses in thrust occurred on the outboard blade sections owing to flow breakdown; the load on the inboard sections increased slightly.

Aircraft Engine Research Laboratory,
National Advisory Committee for Aeronautics,
Cleveland, Ohio.

Martin J. Saari,
Aeronautical Engineer.

Solomon M. Sorin,
Mechanical Engineer.

Approved:
Alfred W. Young,
Mechanical Engineer.

Abe Silverstein,
Aeronautical Engineer.

vab

REFERENCES

1. Saari, Martin J., and Wallner, Lewis E.: Altitude-Wind-Tunnel Investigation of Performance of Several Propellers on YP-47M Airplane at High Blade Loading. I - Aeroproducts H20C-162-X11M2 Four-Blade Propeller. NACA RM No. E6I24, Army Air Forces, 1946.

2. Wallner, Lewis E., and Sorin, Solomon M.: Altitude-Wind-Tunnel Investigation of Performance of Several Propellers on YP-47M Airplane at High Blade Loading. II - Curtiss 838-1C2-18R1 Four-Blade Propeller. NACA RM No. E6J14, Army Air Forces, 1946.

3. Saari, Martin J., and Converse, Arthur M.: Altitude-Wind-Tunnel Investigation of Performance of Several Propellers on YP-47M Airplane at High Blade Loadings. III - Hamilton Standard A6543A-0 Four-Blade Propeller. NACA RM No. E6J22, Army Air Forces, 1946.

4. Saari, Martin J., and Sorin, Solomon M.: Altitude-Wind-Tunnel Investigation of Performance of Several Propellers on YP-47M Airplane at High Blade Loadings. IV - Curtiss 732-1C2-0 Four-Blade Propeller. NACA RM No. E6J23, Army Air Forces, 1946.

5. Saari, Martin J., and Wallner, Lewis E.: Altitude-Wind-Tunnel Investigation of Several Propellers on YP-47M Airplane at High Blade Loadings. V - Curtiss 836-14C2-18R1 Four-Blade Propeller. NACA RM No. E6J31, Army Air Forces, 1946.

6. Pendley, Robert E.: Effect of Propeller-Axis Angle of Attack on Thrust Distribution over the Propeller Disk in Relation to Wake-Survey Measurement of Thrust. NACA ARR No. L5J02b, 1945.

INDEX OF FIGURES

Figure 9. - Effect of advance-diameter ratio J on blade thrust load distribution at power coefficient C_p of approximately 0.40 and free-stream Mach number M_o of approximately 0.20. Hamilton Standard 6507A-2 four-blade propeller.
(a) C_p, 0.38; J, 1.05; M_o, 0.19; M_t, 0.60.
(b) C_p, 0.40; J, 0.81; M_o, 0.20; M_t, 0.79.

Figure 10. - Effect of advance-diameter ratio J on blade thrust load distribution at power coefficient C_p of approximately 0.80 and free-stream Mach number M_o of approximately 0.20. Hamilton Standard 6507A-2 four-blade propeller.
(a) C_p, 0.79; J, 1.55; M_o, 0.20; M_t, 0.45.
(b) C_p, 0.76; J, 1.43; M_o, 0.20; M_t, 0.48.
(c) C_p, 0.83; J, 1.31; M_o, 0.18; M_t, 0.48.
(d) C_p, 0.81; J, 0.99; M_o, 0.17; M_t, 0.58.

Figure 11. - Characteristics of Hamilton Standard 6507A-2 four-blade propeller on YP-47M airplane at free-stream Mach number M_o of approximately 0.30.

Figure 12. - Effect of power coefficient C_p on blade thrust load distribution at advance-diameter ratio J of approximately 1.30 and free-stream Mach number M_o of approximately 0.30. Hamilton Standard 6507A-2 four-blade propeller.
(a) C_p, 0.09; J, 1.29; M_o, 0.30; M_t, 0.78.
(b) C_p, 0.19; J, 1.30; M_o, 0.30; M_t, 0.78.
(c) C_p, 0.50; J, 1.21; M_o, 0.30; M_t, 0.82.

Figure 13. - Effect of advance-diameter ratio J on blade thrust load distribution at power coefficient C_p of approximately 0.20 and free-stream Mach number M_o of approximately 0.30. Hamilton Standard 6507A-2 four-blade propeller.
(a) C_p, 0.17; J, 1.67; M_o, 0.31; M_t, 0.65.
(b) C_p, 0.19; J, 1.30; M_o, 0.30; M_t, 0.78.
(c) C_p, 0.21; J, 0.96; M_o, 0.28; M_t, 0.96.

Figure 14. - Effect of advance-diameter ratio J on blade thrust load distribution at power coefficient C_p of approximately 0.40 and free-stream Mach number M_o of approximately 0.30. Hamilton Standard 6507A-2 four-blade propeller.
(a) C_p, 0.37; J, 2.02; M_o, 0.30; M_t, 0.55.
(b) C_p, 0.39; J, 1.60; M_o, 0.30; M_t, 0.65.
(c) C_p, 0.41; J, 1.17; M_o, 0.28; M_t, 0.81.
(d) C_p, 0.42; J, 1.00; M_o, 0.29; M_t, 0.96.

Figure 15. - Effect of advance-diameter ratio J on blade thrust load distribution at power coefficient C_p of approximately 0.50 and free-stream Mach number M_o of approximately 0.30. Hamilton Standard 6507A-2 four-blade propeller.
(a) C_p, 0.47; J, 2.02; M_o, 0.30; M_t, 0.55.
(b) C_p, 0.50; J, 1.56; M_o, 0.29; M_t, 0.65.
(c) C_p, 0.50; J, 1.21; M_o, 0.30; M_t, 0.82.

Figure 16. - Characteristics of Hamilton Standard 6507A-2 four-blade propeller on YP-47M airplane at free-stream Mach number M_o of approximately 0.40.

Figure 17. - Effect of power coefficient C_p on blade thrust load distribution at advance-diameter ratio J of approximately 2.10 and free-stream Mach number M_o of approximately 0.40. Hamilton Standard 6507A-2 four-blade propeller.
(a) C_p, 0.09; J, 2.05; M_o, 0.39; M_t, 0.71.
(b) C_p, 0.38; J, 2.20; M_o, 0.39; M_t, 0.68.
(c) C_p, 0.48; J, 2.20; M_o, 0.39; M_t, 0.68.
(d) C_p, 0.61; J, 2.15; M_o, 0.40; M_t, 0.71.
(e) C_p, 0.99; J, 2.03; M_o, 0.38; M_t, 0.70.

Figure 18. - Characteristics of Hamilton Standard 6507A-2 three-blade propeller on YP-47M airplane at free-stream Mach number M_o of approximately 0.40.

Figure 19. - Effect of power coefficient C_p on blade thrust load distribution at advance-diameter ratio J of approximately 1.75 and free-stream Mach number M_o of approximately 0.40. Hamilton Standard 6507A-2 three-blade propeller.
(a) C_p, 0.32; J, 1.78; M_o, 0.41; M_t, 0.83.
(b) C_p, 0.53; J, 1.72; M_o, 0.40; M_t, 0.83.
(c) C_p, 0.65; J, 1.78; M_o, 0.39; M_t, 0.80.

Figure 20. - Effect of power coefficient C_p on blade thrust load distribution at advance-diameter ratio J of approximately 2.10 and free-stream Mach number M_o of approximately 0.40. Hamilton Standard 6507A-2 three-blade propeller.
(a) C_p, 0.39; J, 1.97; M_o, 0.40; M_t, 0.76.
(b) C_p, 0.53; J, 2.19; M_o, 0.41; M_t, 0.71.
(c) C_p, 0.63; J, 2.15; M_o, 0.39; M_t, 0.70.
(d) C_p, 0.74; J, 2.11; M_o, 0.39; M_t, 0.69.
(e) C_p, 0.85; J, 2.09; M_o, 0.38; M_t, 0.69.
(f) C_p, 0.94; J, 2.03; M_o, 0.37; M_t, 0.69.
(g) C_p, 1.07; J, 2.05; M_o, 0.37; M_t, 0.68.

Figure 21. - Effect of power coefficient C_p on blade thrust load distribution at advance-diameter ratio J of approximately 2.90 and free-stream Mach number M_o of approximately 0.40. Hamilton Standard 6507A-2 three-blade propeller.
(a) C_p, 0.62; J, 2.87; M_o, 0.40; M_t, 0.59.
(b) C_p, 0.75; J, 2.90; M_o, 0.40; M_t, 0.59.
(c) C_p, 0.85; J, 2.89; M_o, 0.40; M_t, 0.59.
(d) C_p, 1.03; J, 2.72; M_o, 0.39; M_t, 0.60.

Figure 22. - Effect of advance-diameter ratio J on blade thrust load distribution at power coefficient C_p of approximately 0.32 and free-stream Mach number M_o of approximately 0.40. Hamilton Standard 6507A-2 three-blade propeller.
(a) C_p, 0.32; J, 3.06; M_o, 0.40; M_t, 0.57.
(b) C_p, 0.32; J, 2.36; M_o, 0.39; M_t, 0.66.
(c) C_p, 0.32; J, 1.97; M_o, 0.40; M_t, 0.76.
(d) C_p, 0.32; J, 1.78; M_o, 0.41; M_t, 0.83.
(e) C_p, 0.32; J, 1.44; M_o, 0.40; M_t, 0.97.

Figure 23. - Effect of advance-diameter ratio J on blade thrust load distribution at power coefficient C_p of approximately 0.53 and free-stream Mach number M_o of approximately 0.40. Hamilton Standard 6507A-2 three-blade propeller.
(a) C_p, 0.53; J, 3.32; M_o, 0.40; M_t, 0.55.
(b) C_p, 0.53; J, 2.53; M_o, 0.40; M_t, 0.64.
(c) C_p, 0.53; J, 2.19; M_o, 0.41; M_t, 0.71.
(d) C_p, 0.53; J, 1.72; M_o, 0.40; M_t, 0.83.

Figure 24. - Effect of advance-diameter ratio J on blade thrust load distribution at power coefficient C_p of approximately 0.63 and free-stream Mach number M_o of approximately 0.40. Hamilton Standard 6507A-2 three-blade propeller.
(a) C_p, 0.64; J, 3.60; M_o, 0.40; M_t, 0.53.
(b) C_p, 0.62; J, 2.87; M_o, 0.40; M_t, 0.59.
(c) C_p, 0.63; J, 2.15; M_o, 0.39; M_t, 0.70.
(d) C_p, 0.65; J, 1.78; M_o, 0.39; M_t, 0.80.

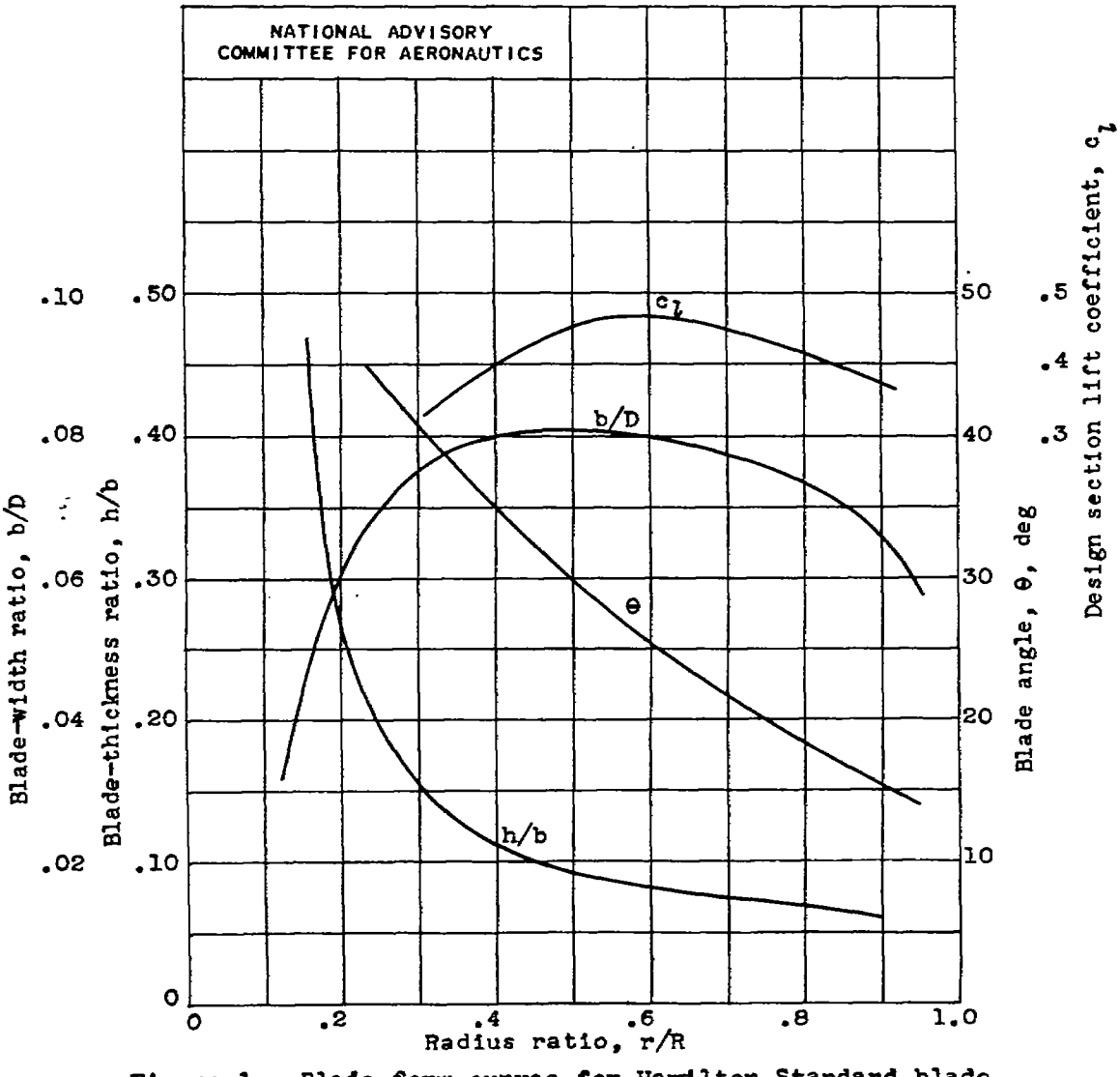

Figure 1.- Blade-form curves for Hamilton Standard blade design 6507A-2. b, section chord; D, propeller diameter; h, section thickness; R, radius to tip; r, section radius.

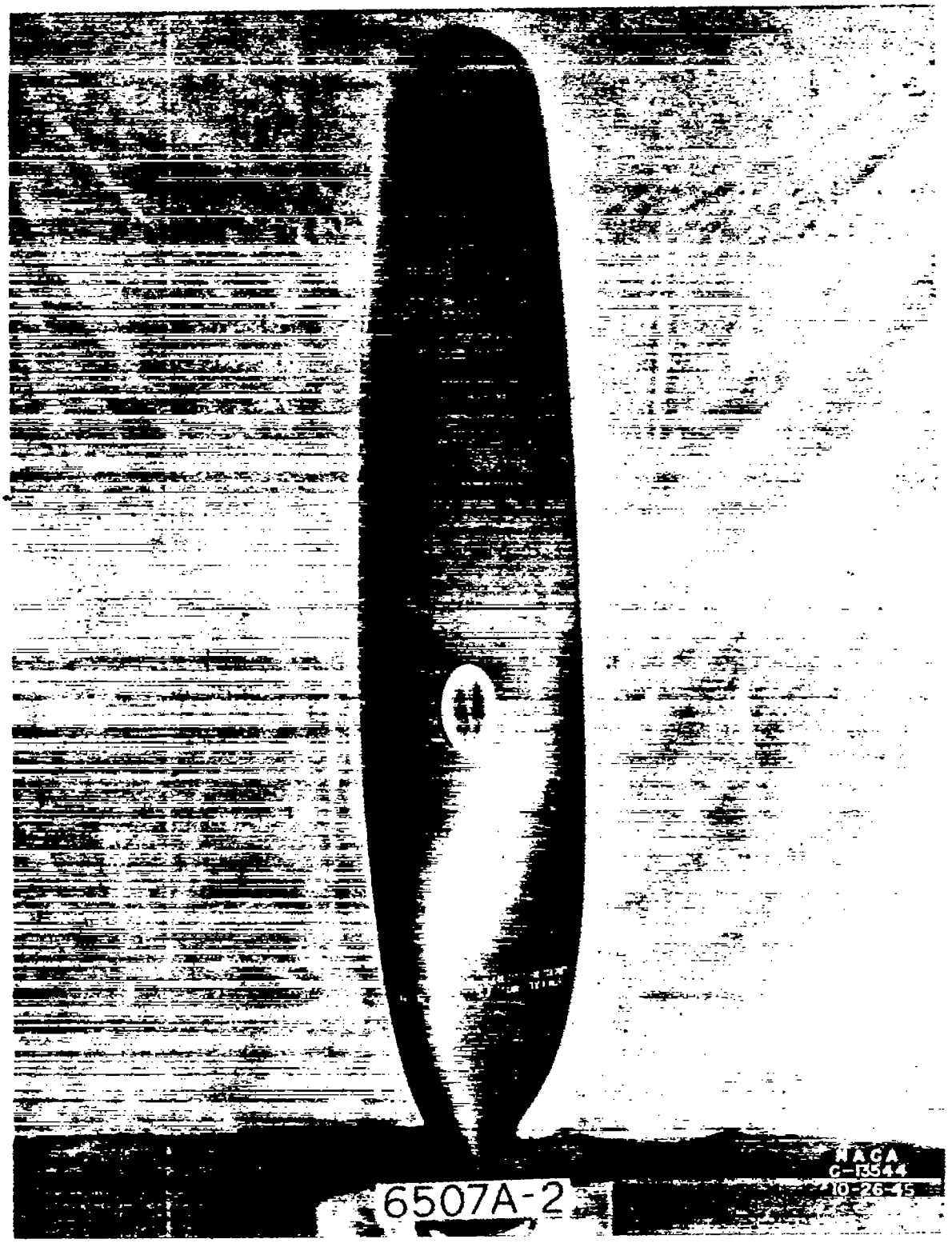

Figure 2. - Hamilton Standard 6507A-2 propeller blade.

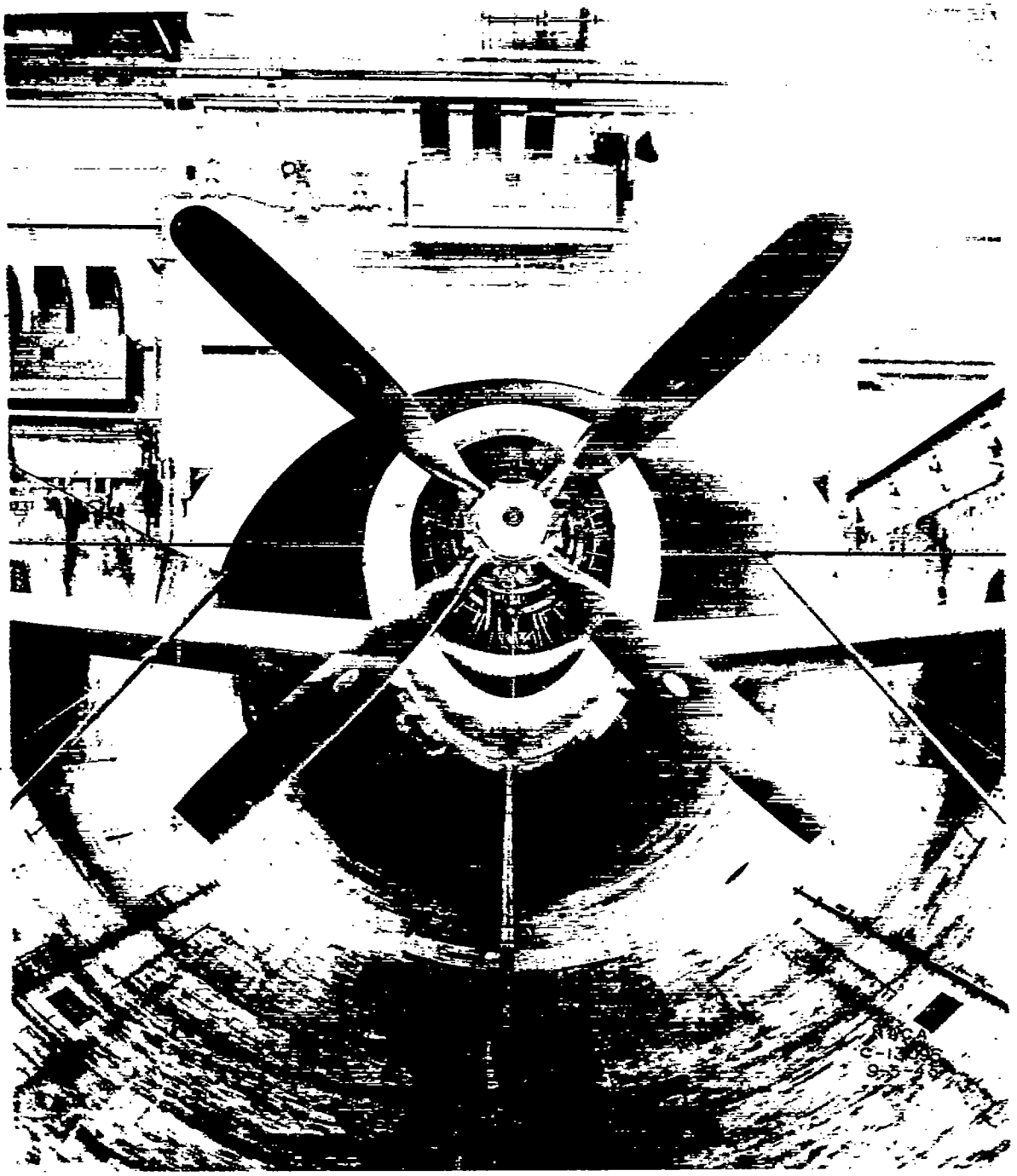

Figure 3. - Front view of YP-47M airplane with Hamilton Standard 6507A-2 four-blade propeller installed in altitude-wind-tunnel test section.

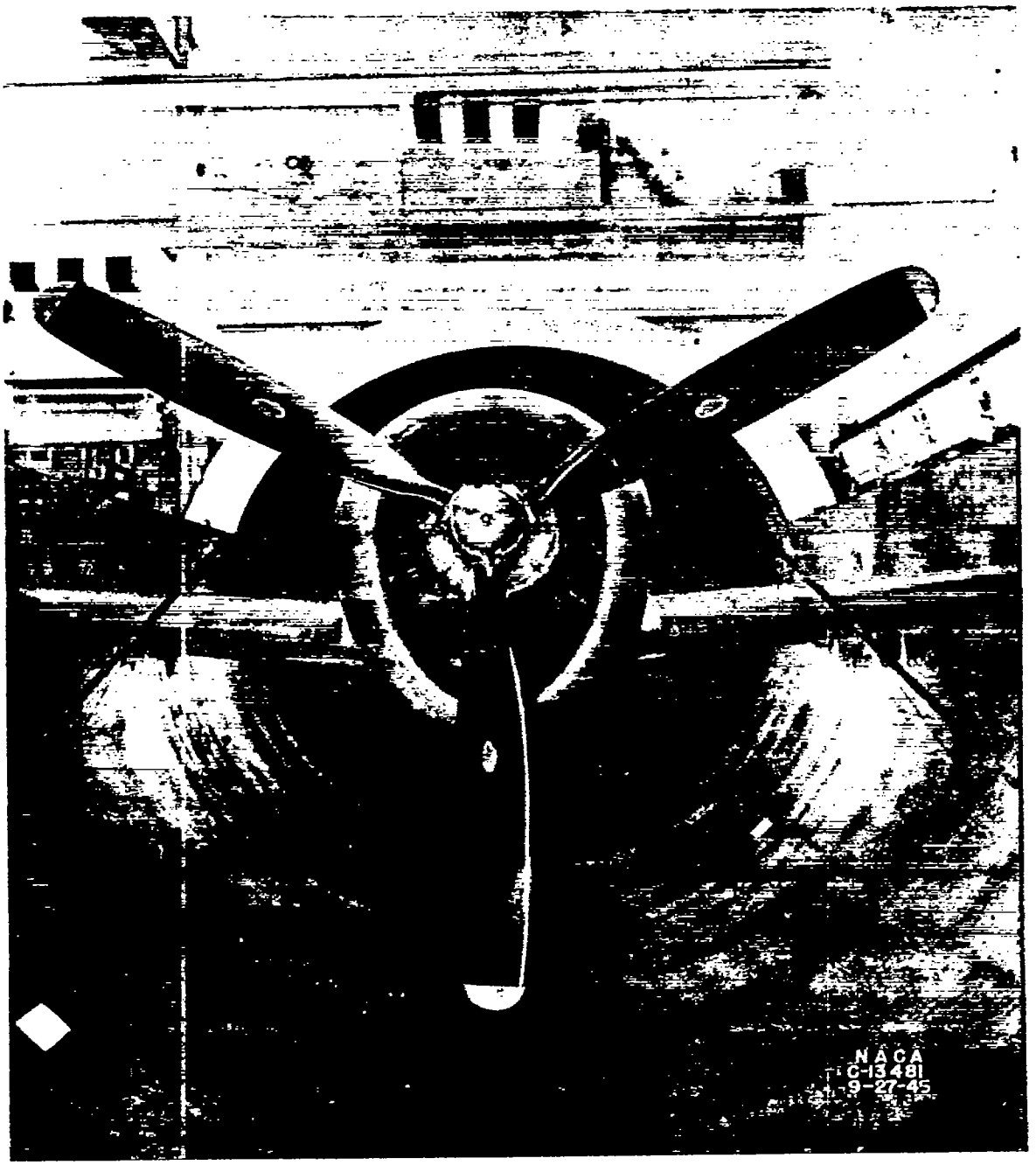

Figure 4. - Front view of YP-47M airplane with Hamilton Standard 6507A-2 three-blade propeller installed in altitude-wind-tunnel test section.

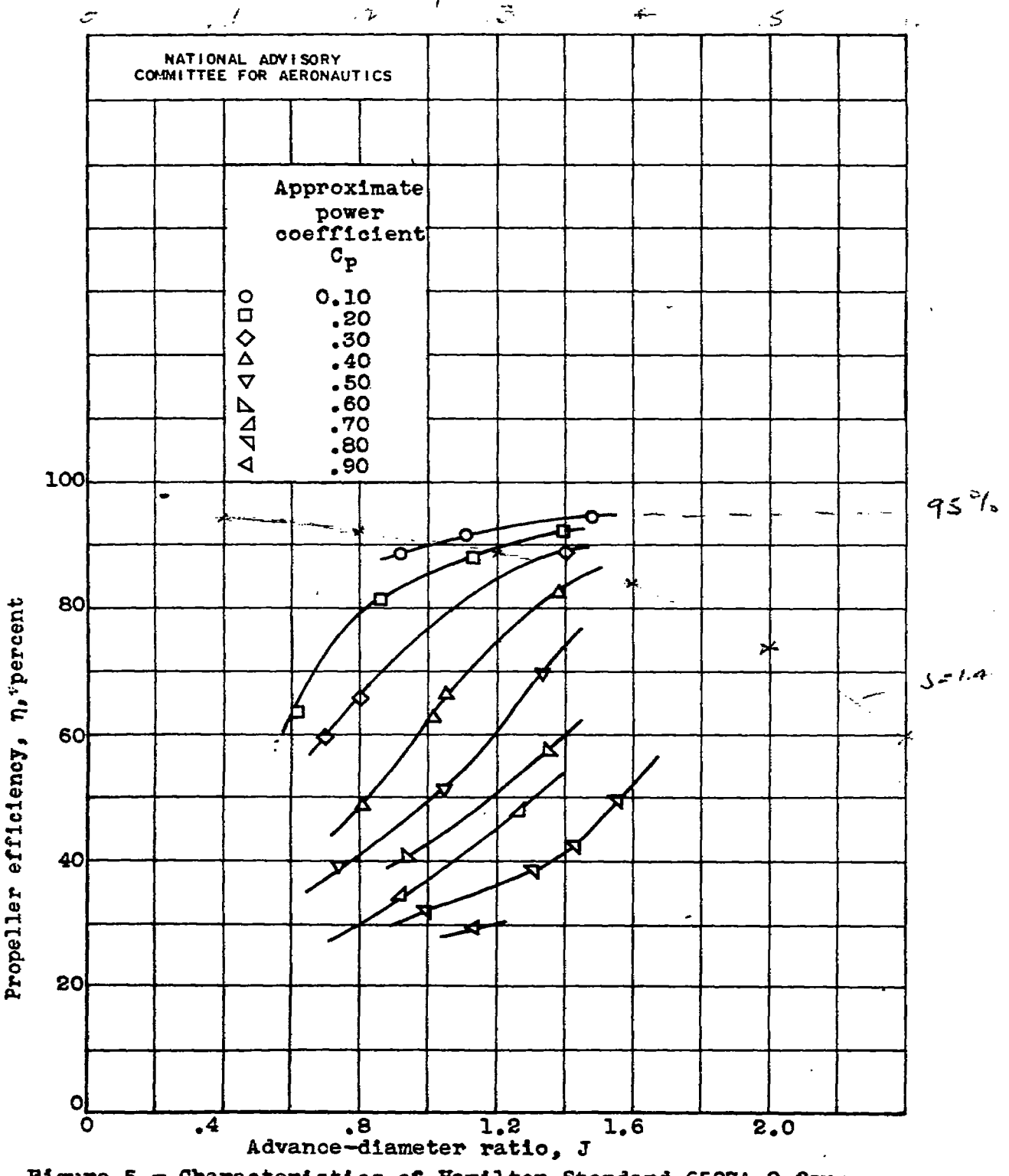

Figure 5.- Characteristics of Hamilton Standard 6507A-2 four-blade propeller on YP-47M airplane at free-stream Mach number M_o of approximately 0.20.

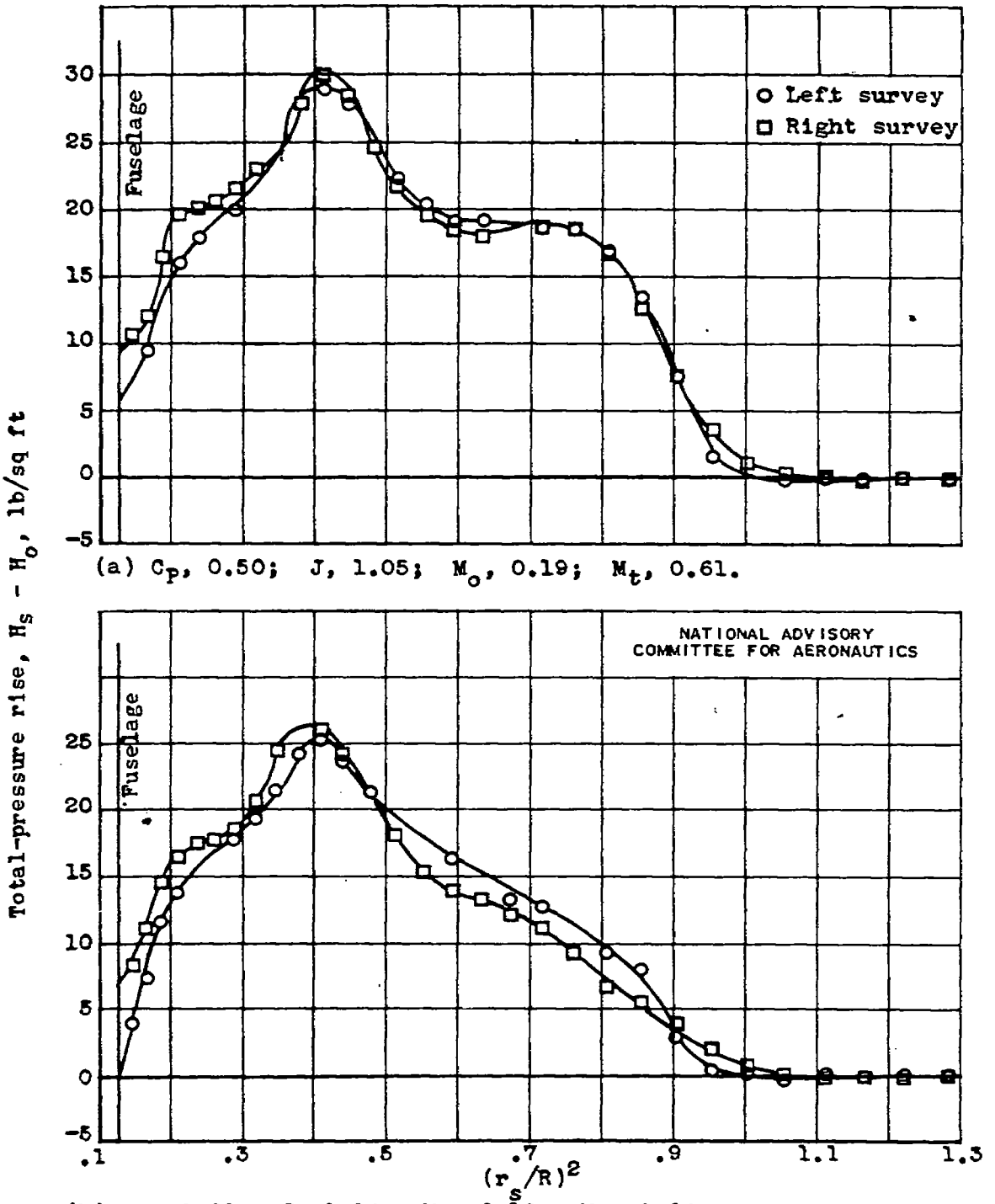

(a) C_p, 0.50; J, 1.05; M_o, 0.19; M_t, 0.61.

(b) C_p, 0.60; J, 0.94; M_o, 0.18; M_t, 0.64.

Figure 6.- Effect of power coefficient C_p on blade thrust load distribution at advance-diameter ratio J of approximately 1.00 and free-stream Mach number M_o of approximately 0.20. Hamilton Standard 6507A-2 four-blade propeller.

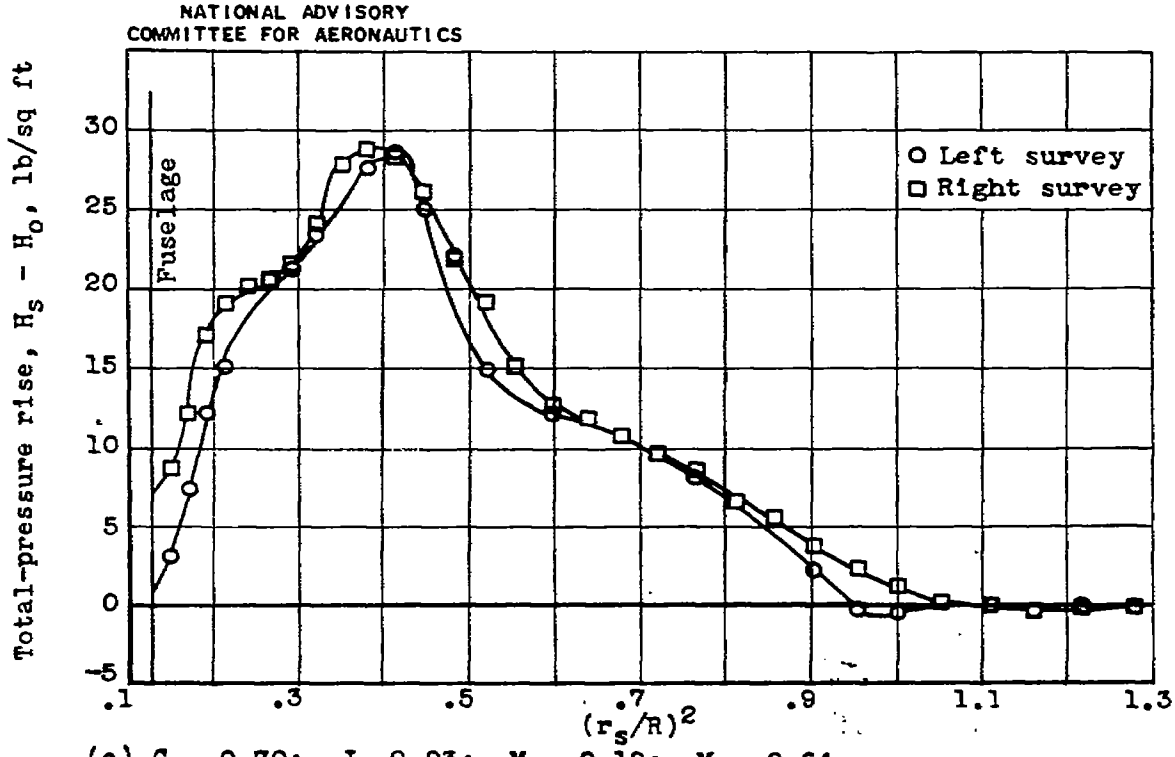

(c) C_p, 0.70; J, 0.93; M_o, 0.18; M_t, 0.64.

Figure 6.- Concluded. Effect of power coefficient C_p on blade thrust load distribution at advance-diameter ratio J of approximately 1.00 and free-stream Mach number M_o of approximately 0.20. Hamilton Standard 6507A-2 four-blade propeller.

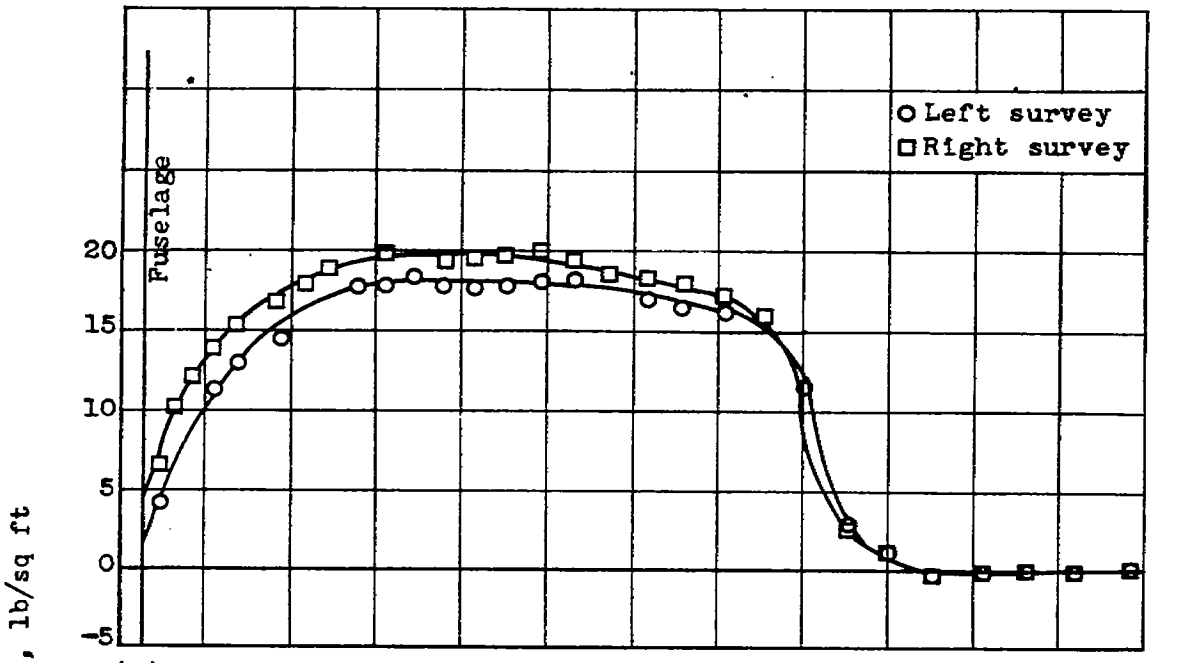

(a) C_p, 0.47; J, 1.33; M_o, 0.19; M_t, 0.49.

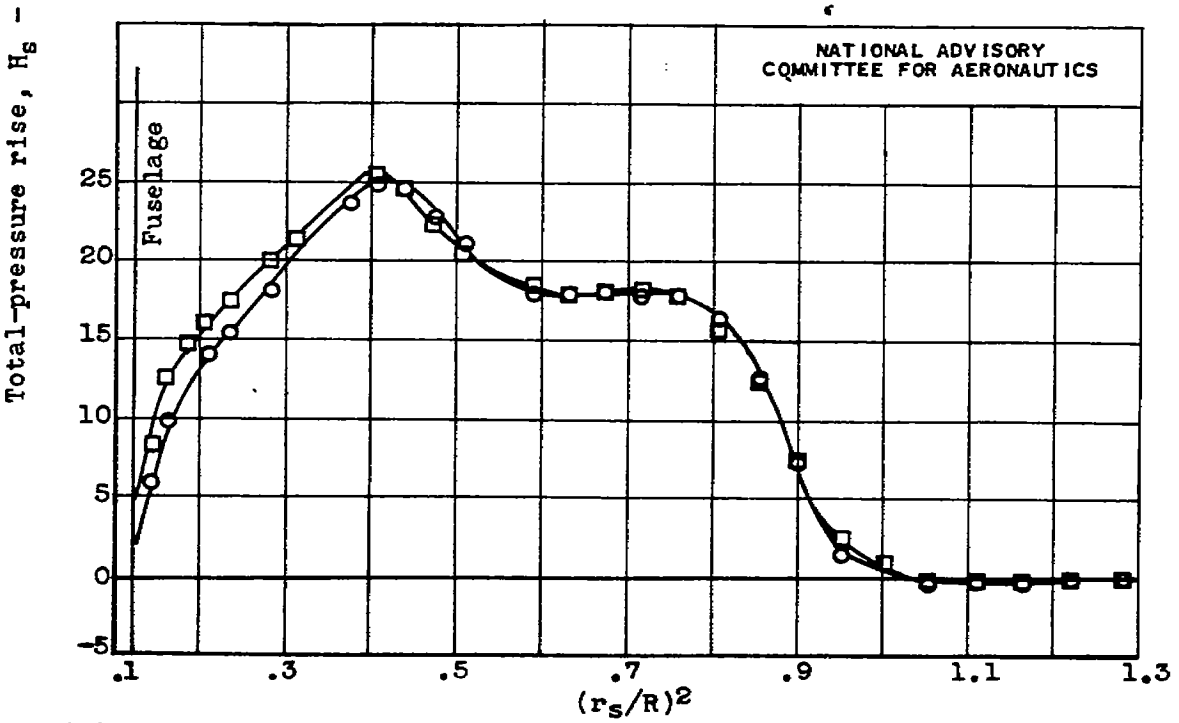

(b) C_p, 0.58; J, 1.35; M_o, 0.19; M_t, 0.49.

Figure 7.- Effect of power coefficient C_p on blade thrust load distribution at advance-diameter ratio J of approximately 1.30 and free-stream Mach number M_o of approximately 0.20. Hamilton Standard 6507A-2 four-blade propeller.

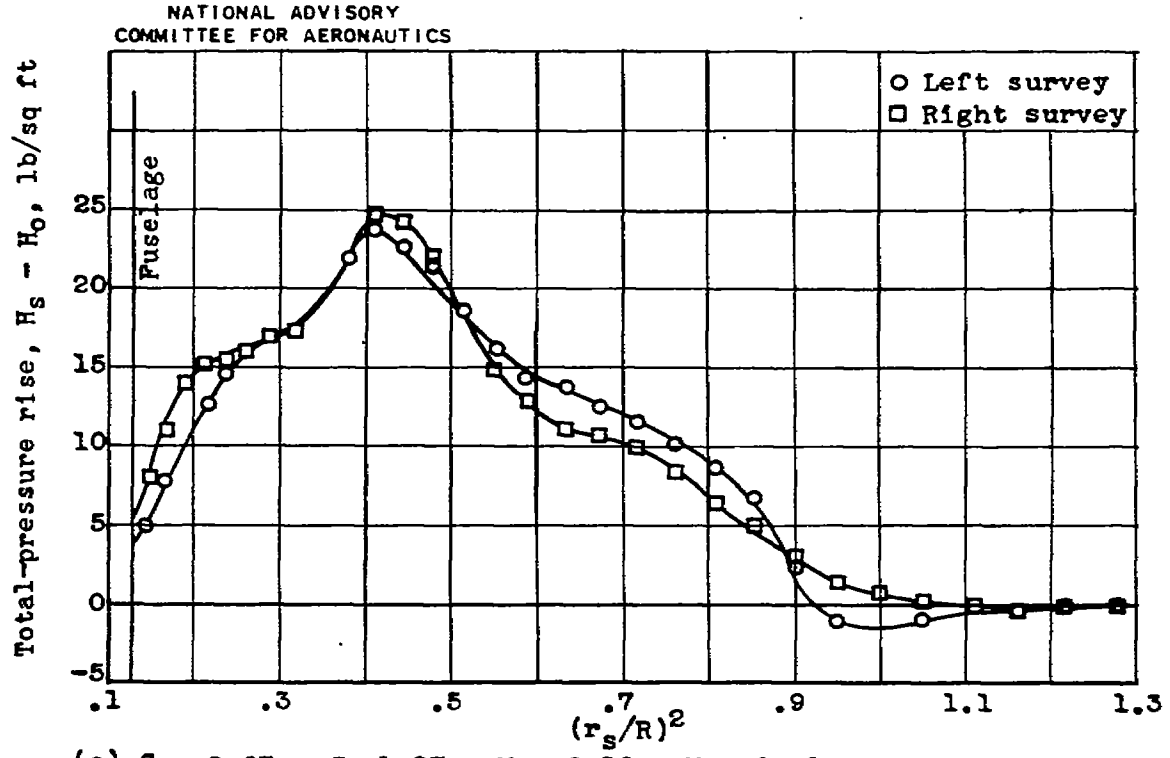

(c) C_p, 0.67; J, 1.27; M_o, 0.19; M_t, 0.51.

Figure 7.- Concluded. Effect of power coefficient C_p on blade thrust load distribution at advance-diameter ratio J of approximately 1.30 and free-stream Mach number M_o of approximately 0.20. Hamilton Standard 6507A-2 four-blade propeller.

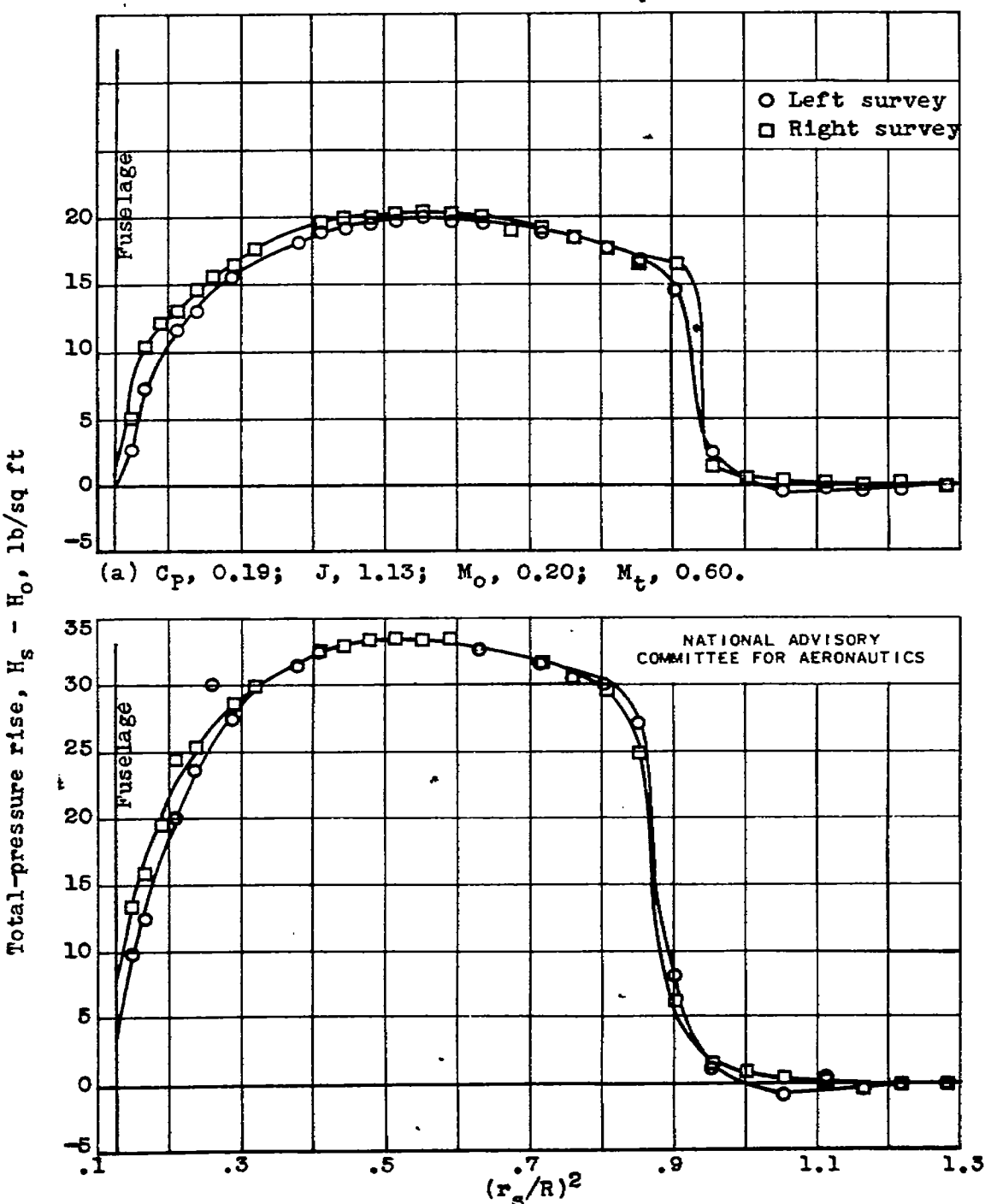

(a) C_p, 0.19; J, 1.13; M_o, 0.20; M_t, 0.60.

(b) C_p, 0.19; J, 0.86; M_o, 0.20; M_t, 0.74.

Figure 8.- Effect of advance-diameter ratio J on blade thrust load distribution at power coefficient C_p of approximately 0.20 and free-stream Mach number M_o of approximately 0.20. Hamilton Standard 6507A-2 four-blade propeller.

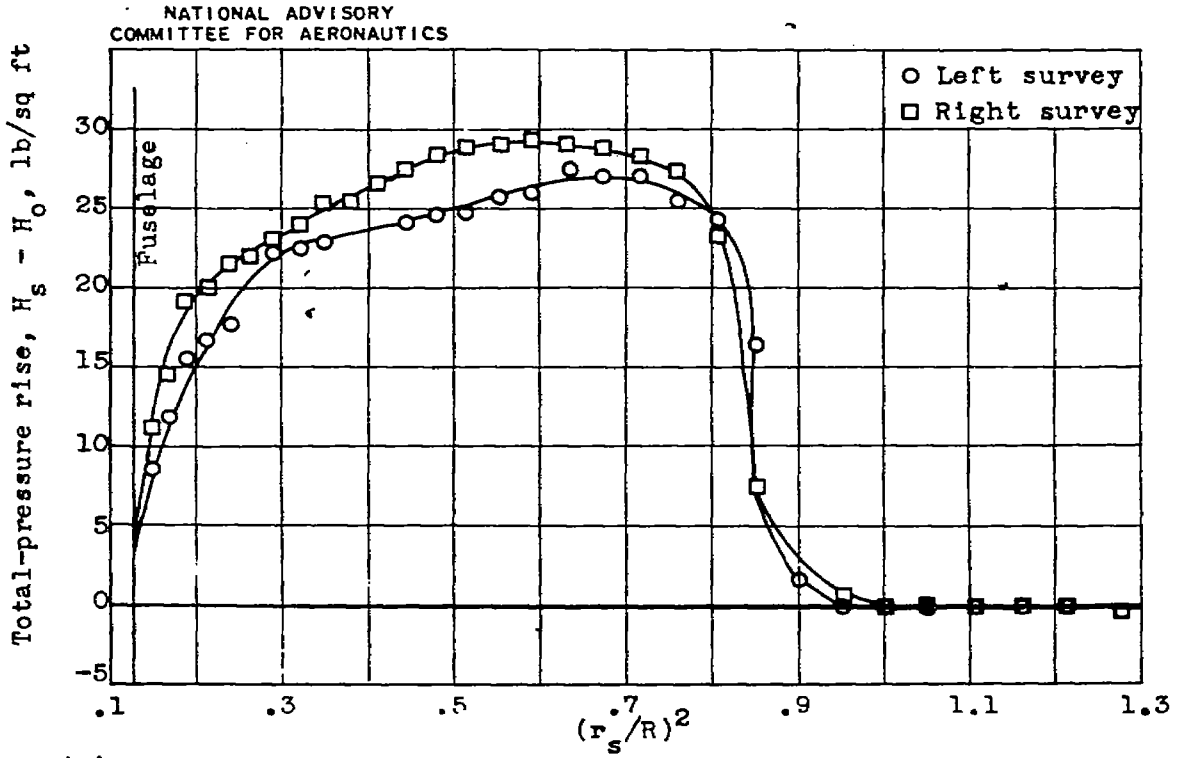

(c) C_p, 0.21; J, 0.62; M_o, 0.18; M_t, 0.93.

Figure 8.- Concluded. Effect of advance-diameter ratio J on blade thrust load distribution at power coefficient C_p of approximately 0.20 and free-stream Mach number M_o of approximately 0.20. Hamilton Standard 6507A-2 four-blade propeller.

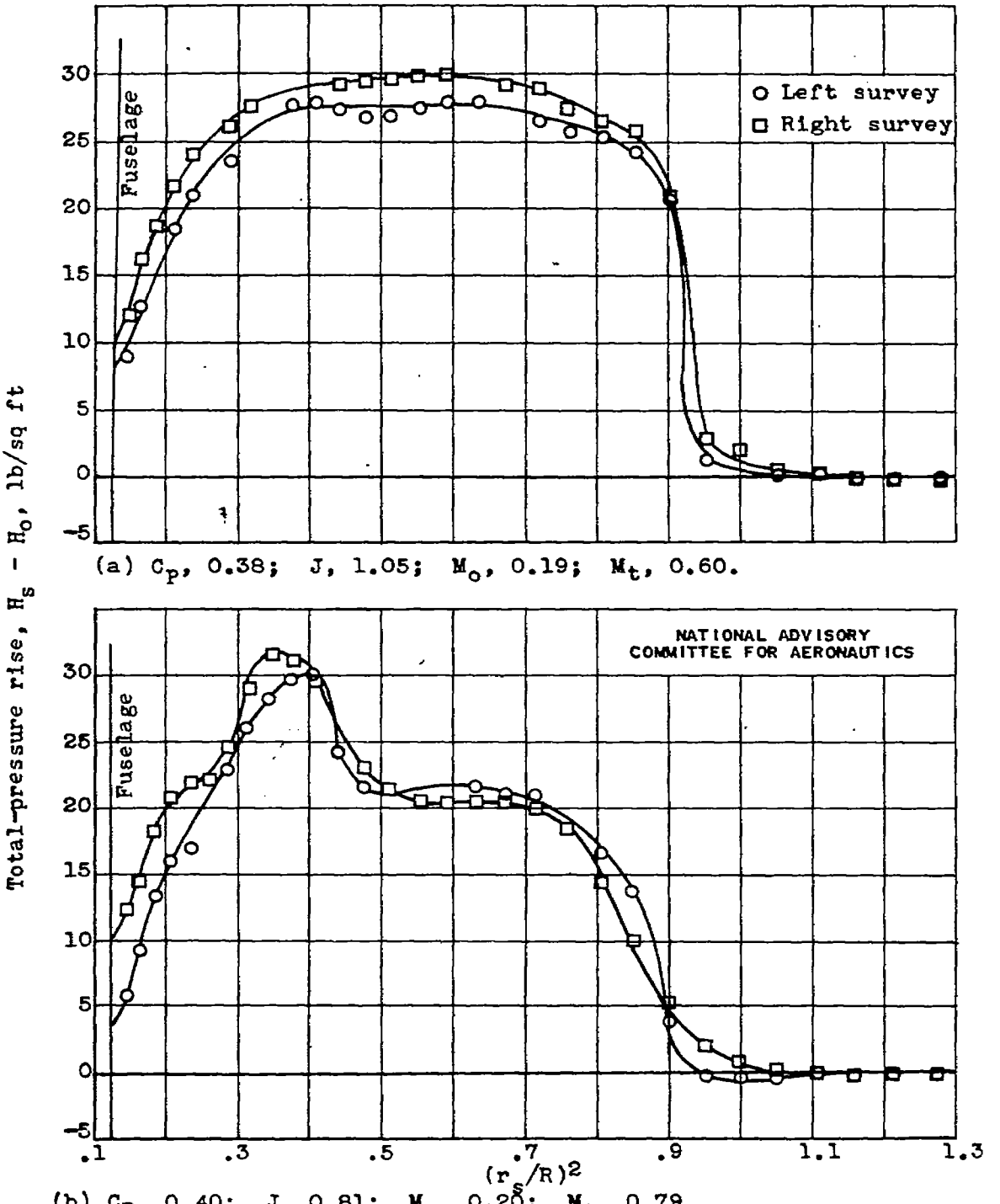

(a) C_p, 0.38; J, 1.05; M_o, 0.19; M_t, 0.60.

(b) C_p, 0.40; J, 0.81; M_o, 0.20; M_t, 0.79.

Figure 9.- Effect of advance-diameter ratio J on blade thrust load distribution at power coefficient C_p of approximately 0.40 and free-stream Mach number M_o of approximately 0.20. Hamilton Standard 6507A-2 four-blade propeller.

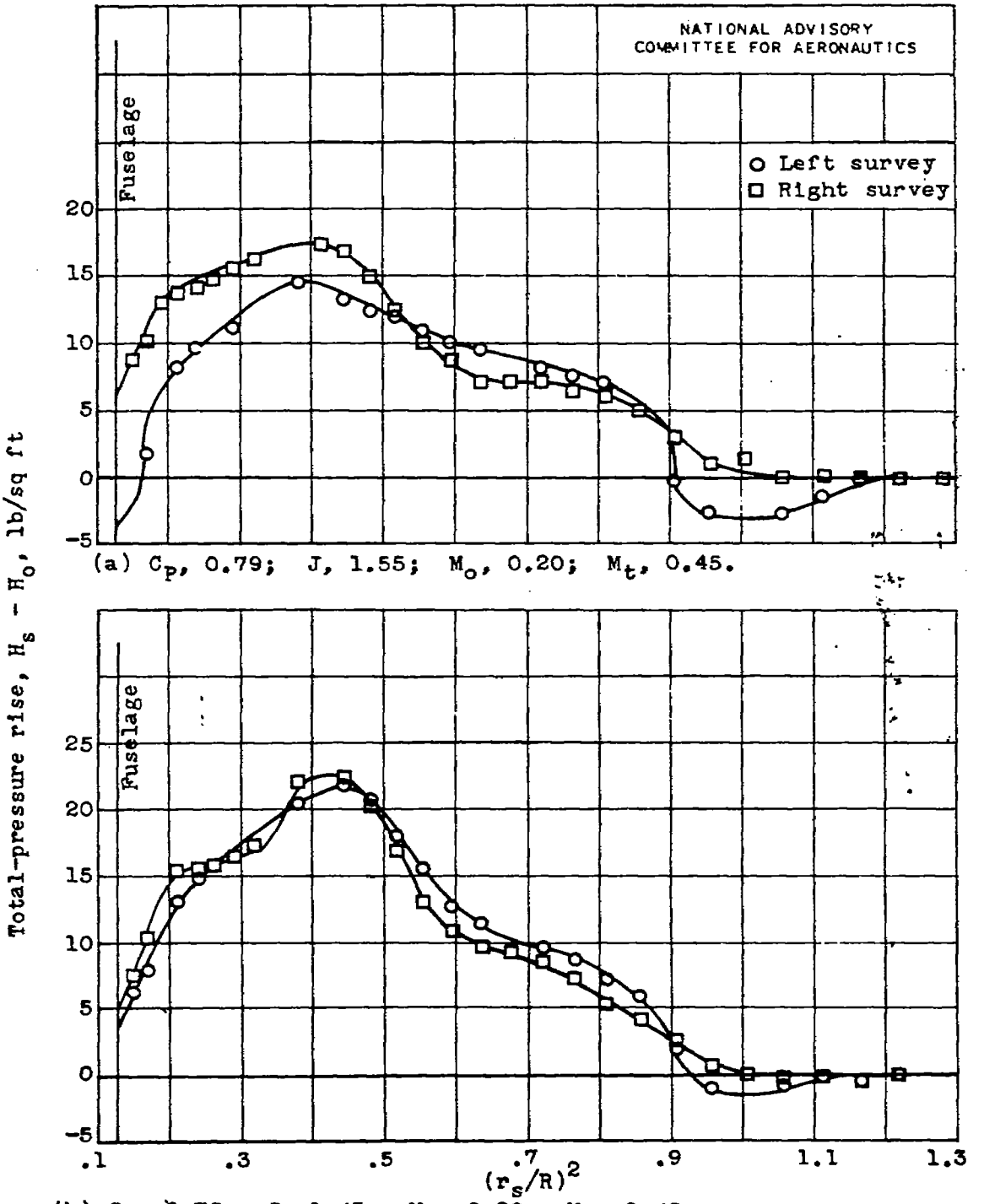

(b) C_p, 0.76; J, 1.43; M_o, 0.20; M_t, 0.48.

Figure 10.- Effect of advance-diameter ratio J on blade thrust load distribution at power coefficient C_p of approximately 0.80 and free-stream Mach number M_o of approximately 0.20. Hamilton Standard 6507A-2 four-blade propeller.

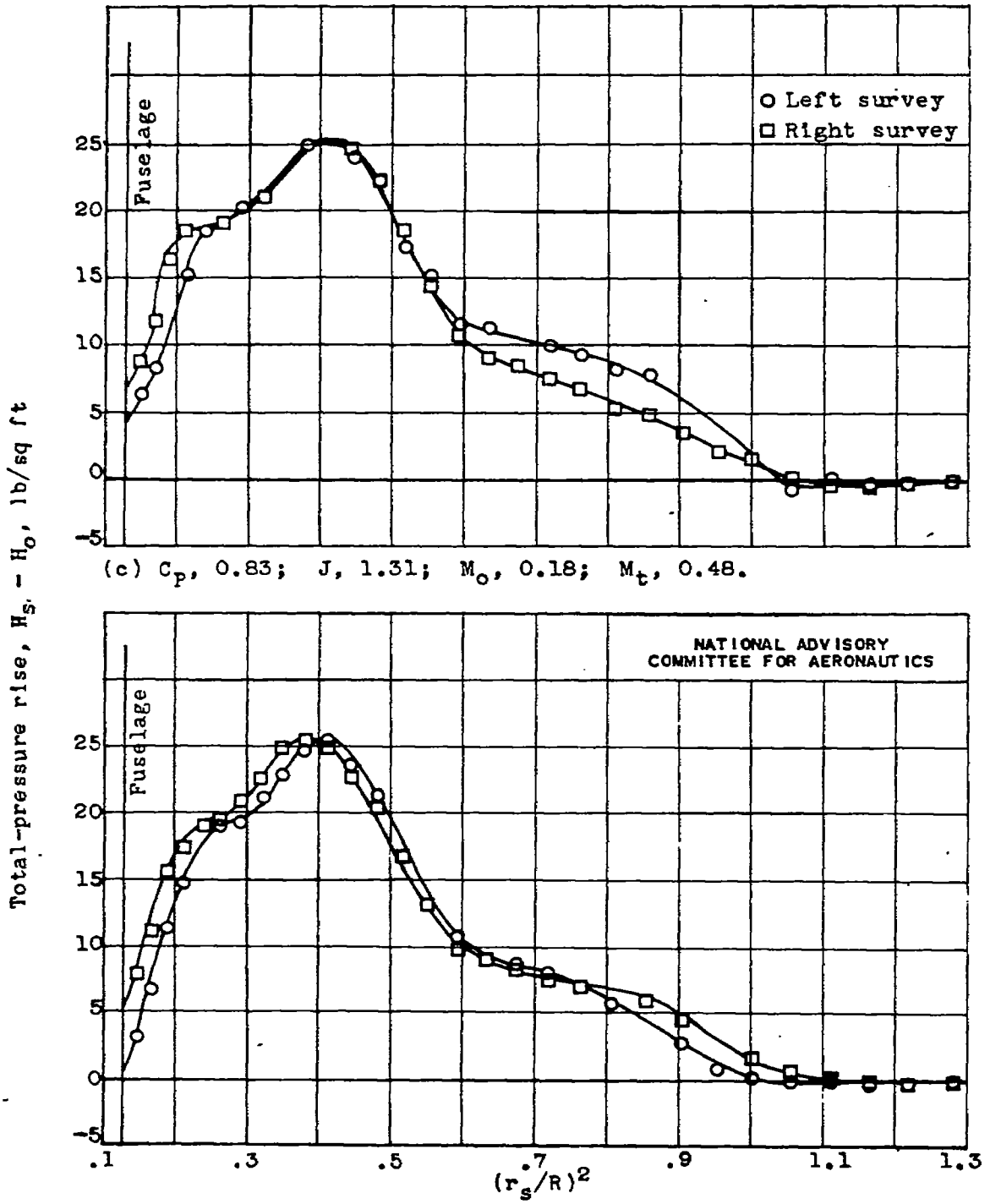

(c) C_p, 0.83; J, 1.31; M_o, 0.18; M_t, 0.48.

(d) C_p, 0.81; J, 0.99; M_o, 0.17; M_t, 0.58.

Figure 10.- Concluded. Effect of advance-diameter ratio J on blade thrust load distribution at power coefficient C_p of approximately 0.80 and free-stream Mach number M_o of approximately 0.20. Hamilton Standard 6507A-2 four-blade propeller.

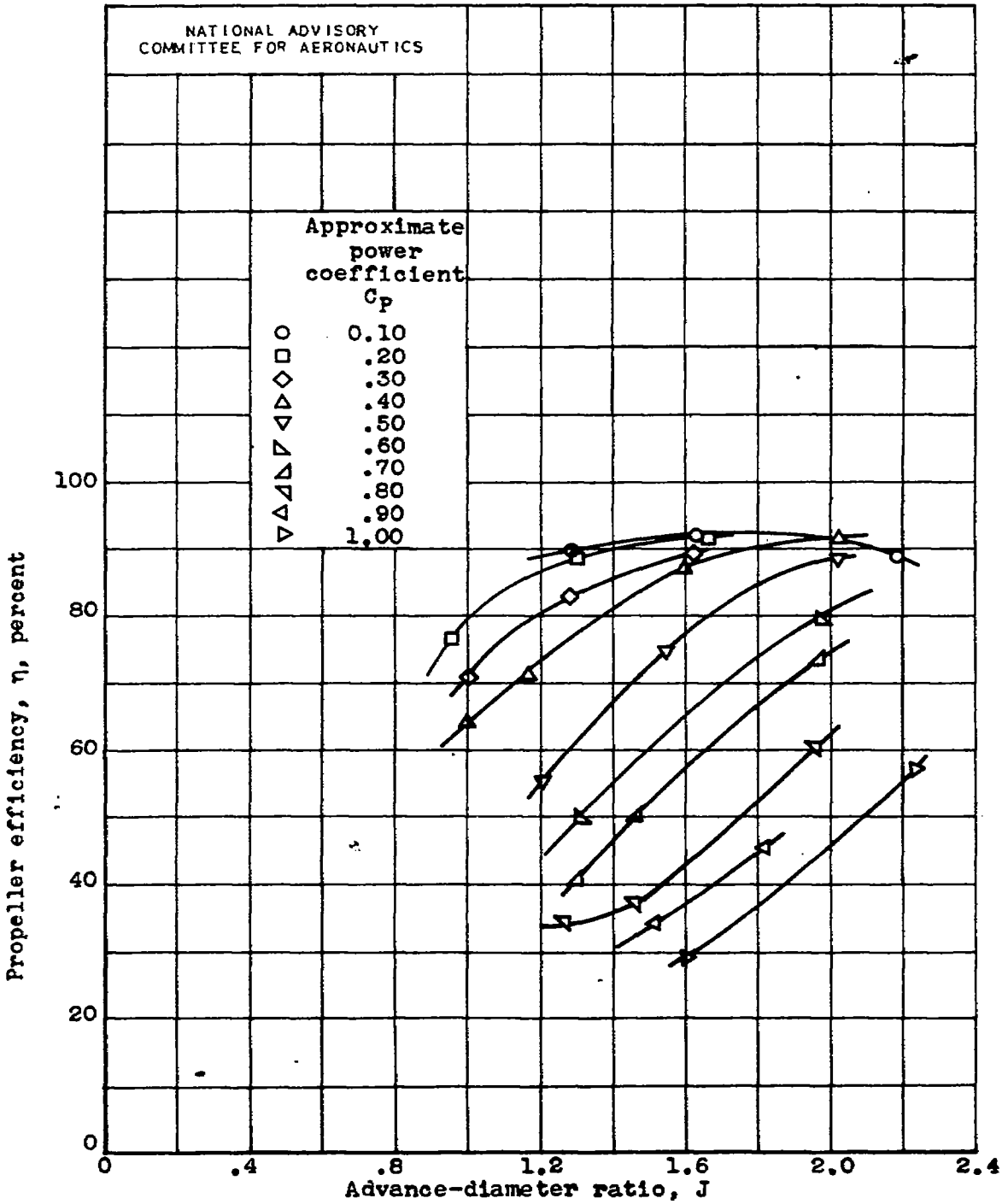

Figure 11.- Characteristics of Hamilton Standard 6507A-2 four-blade propeller on YP-47M airplane at free-stream Mach number M_0 of approximately 0.30.

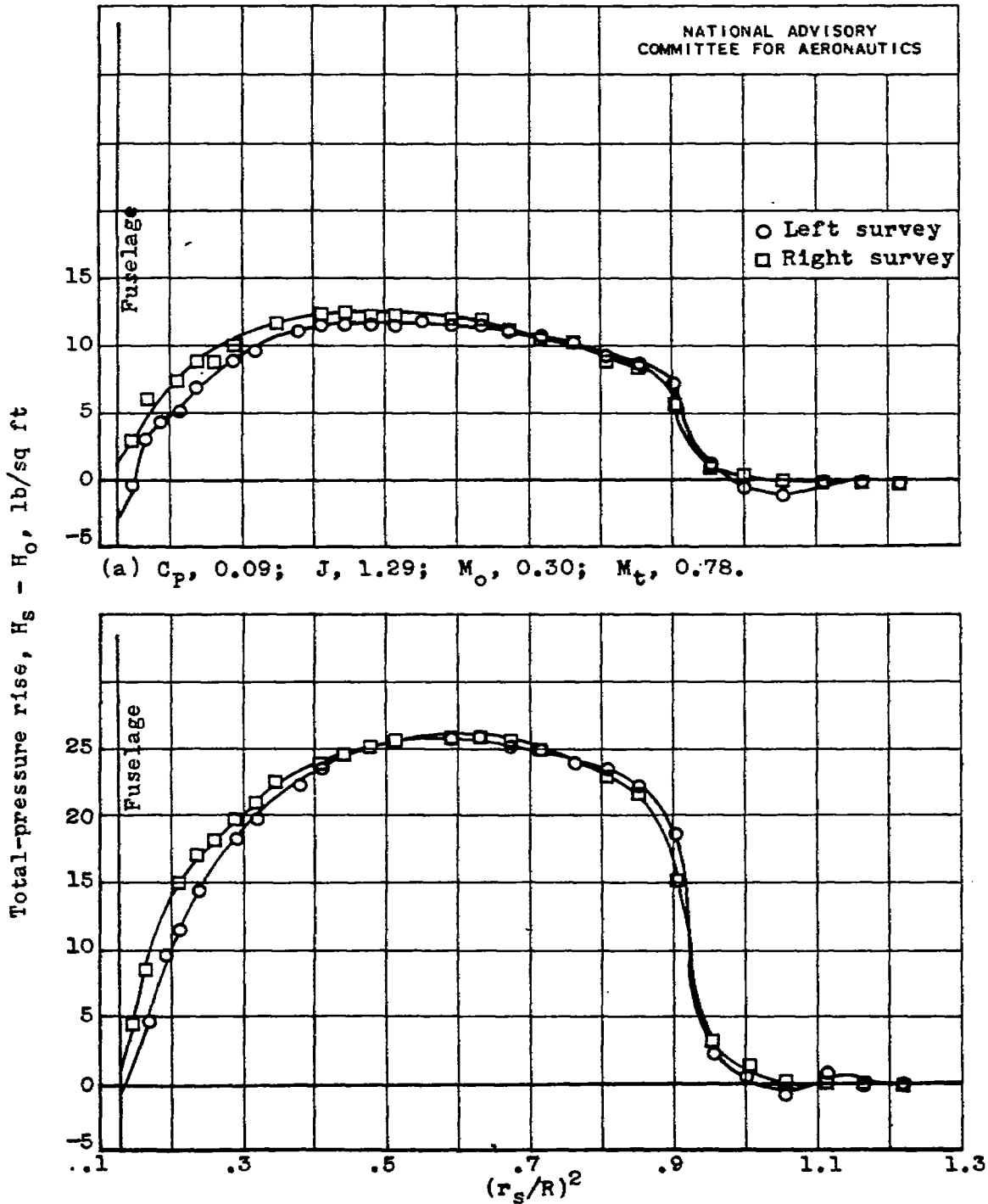

(a) C_p, 0.09; J, 1.29; M_o, 0.30; M_t, 0.78.

(b) C_p, 0.19; J, 1.30; M_o, 0.30; M_t, 0.78.

Figure 12.- Effect of power coefficient C_p on blade thrust load distribution at advance-diameter ratio J of approximately 1.30 and free-stream Mach number M_o of approximately 0.30. Hamilton Standard 6507A-2 four-blade propeller.

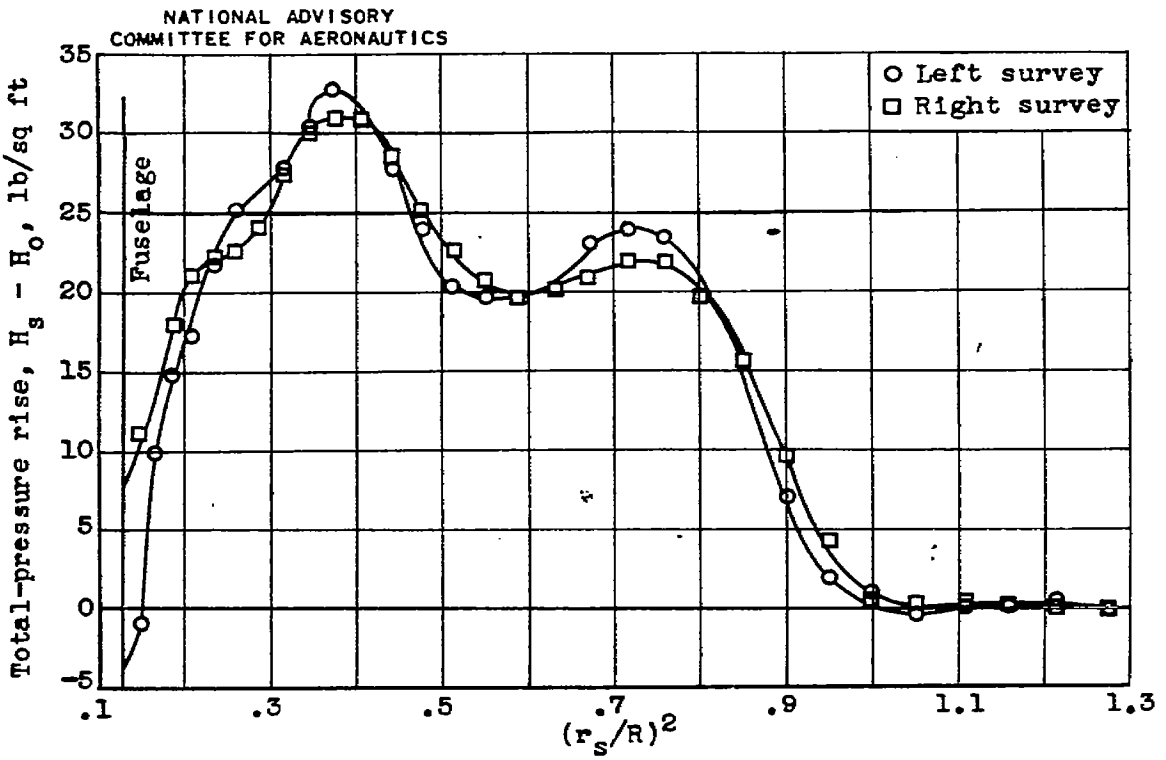

(c) C_p, 0.50; J, 1.21; M_o, 0.30; M_t, 0.82.

Figure 12.- Concluded. Effect of power coefficient C_p on blade thrust load distribution at advance-diameter ratio J of approximately 1.30 and free-stream Mach number M_o of approximately 0.30. Hamilton Standard 6507A-2 four-blade propeller.

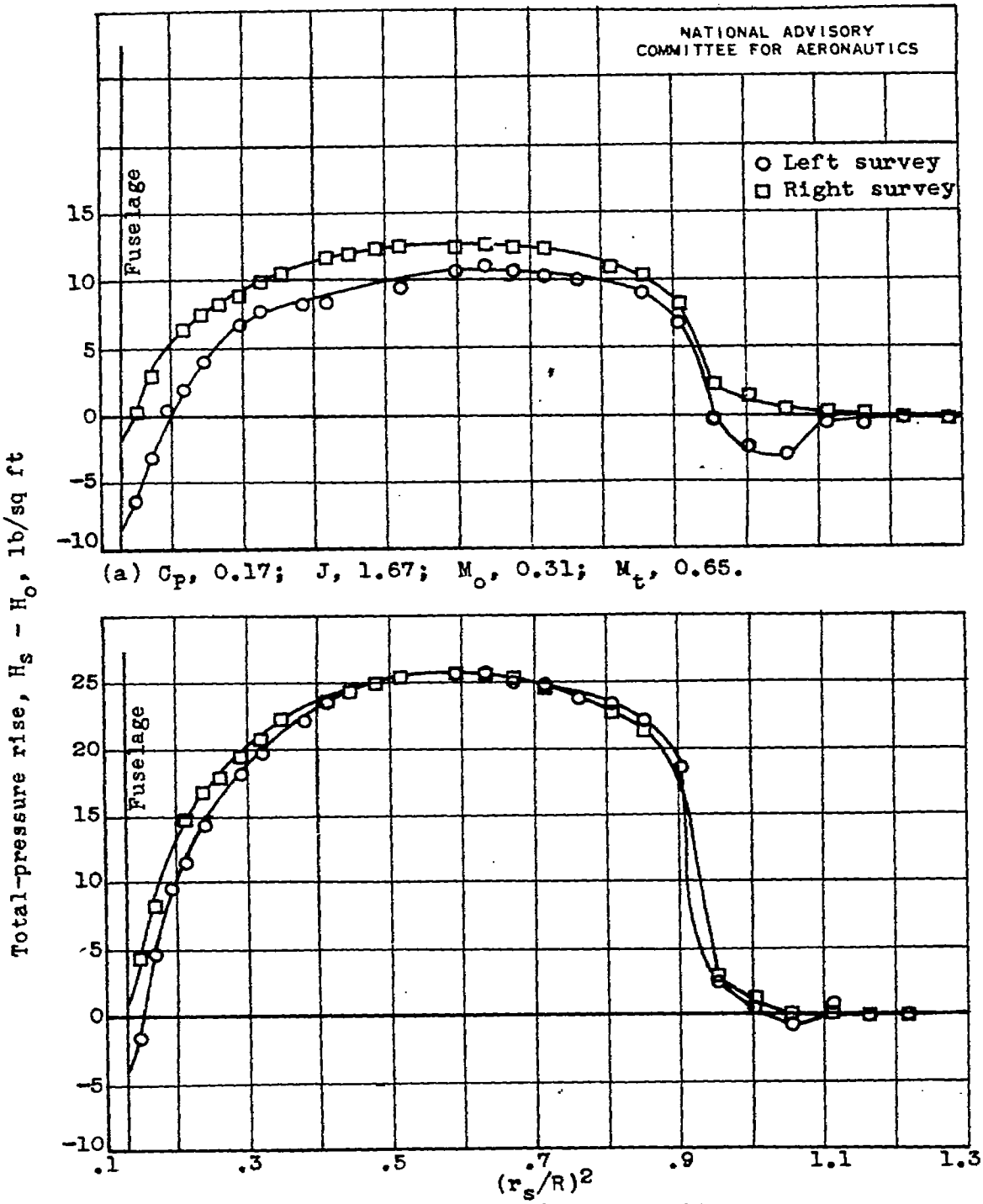

(a) C_p, 0.17; J, 1.67; M_o, 0.31; M_t, 0.65.

(b) C_p, 0.19; J, 1.30; M_o, 0.30; M_t, 0.78.

Figure 13.- Effect of advance-diameter ratio J on blade thrust load distribution at power coefficient C_p of approximately 0.20 and free-stream Mach number M_o of approximately 0.30. Hamilton Standard 6507A-2 four-blade propeller.

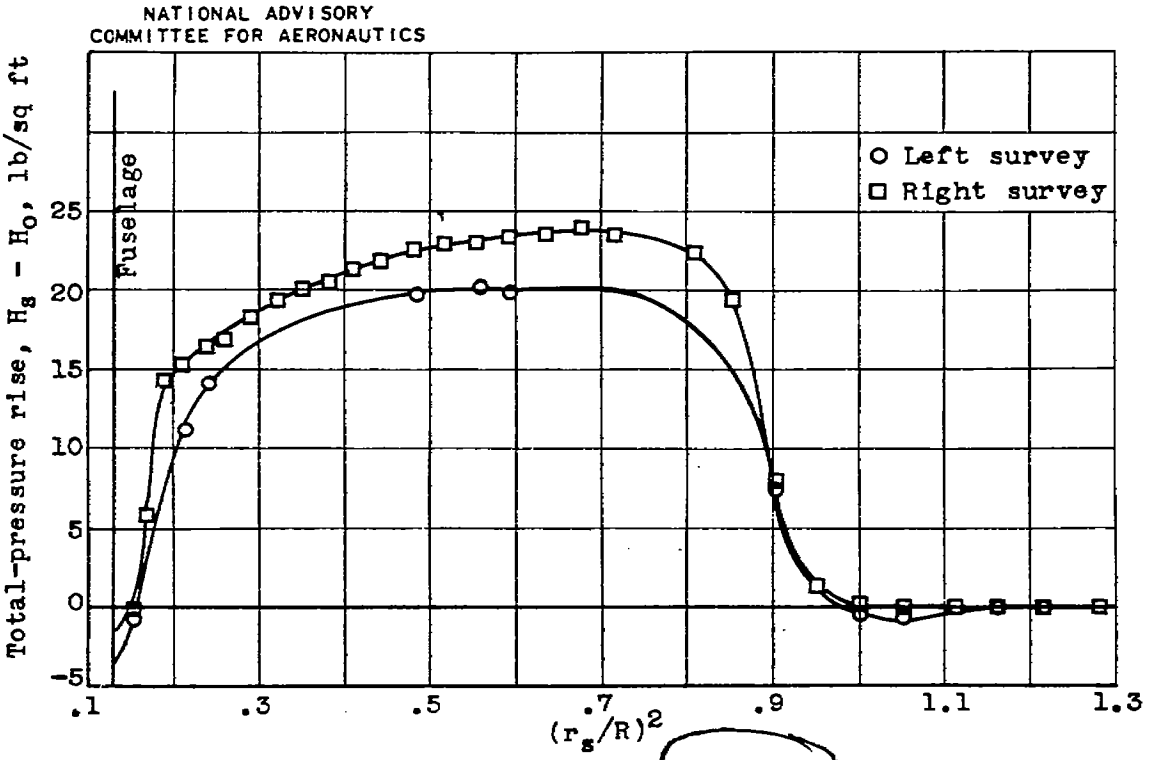

(c) C_P, 0.21; J, 0.96; M_o, 0.28; M_t, 0.96.

Figure 13.- Concluded. Effect of advance-diameter ratio J on blade thrust load distribution at power coefficient C_P of approximately 0.20 and free-stream Mach number M_o of approximately 0.30. Hamilton Standard 6507A-2 four-blade propeller.

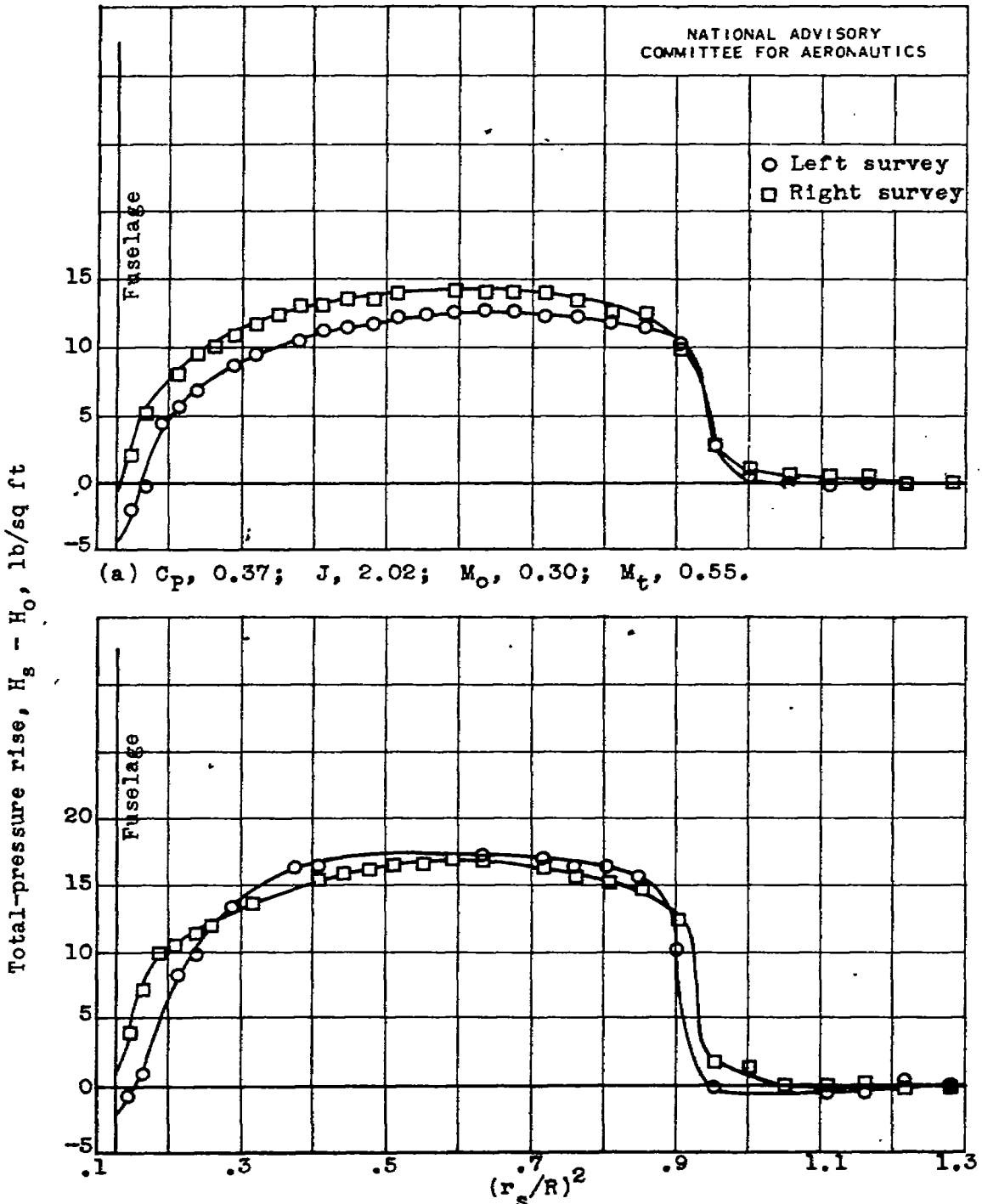

Figure 14.- Effect of advance-diameter ratio J on blade thrust load distribution at power coefficient C_p of approximately 0.40 and free-stream Mach number M_o of approximately 0.30. Hamilton Standard 6507A-2 four-blade propeller.

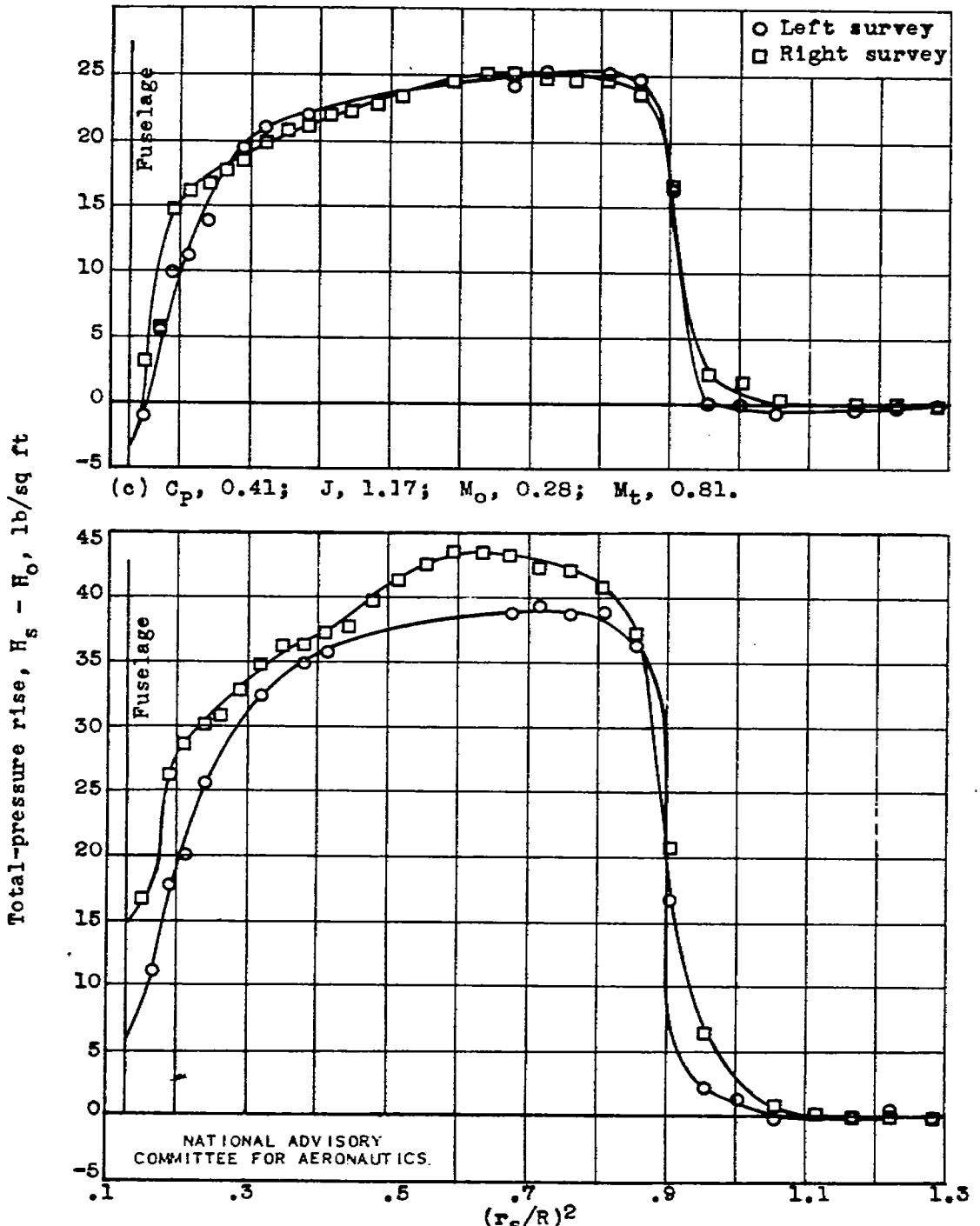

(c) C_p, 0.41; J, 1.17; M_o, 0.28; M_t, 0.81.

(d) C_p, 0.42; J, 1.00; M_o, 0.29; M_t, 0.96.

Figure 14.- Concluded. Effect of advance-diameter ratio J on blade thrust load distribution at power coefficient C_p of approximately 0.40 and free-stream Mach number M_o of approximately 0.30. Hamilton Standard 6507A-2 four-blade propeller.

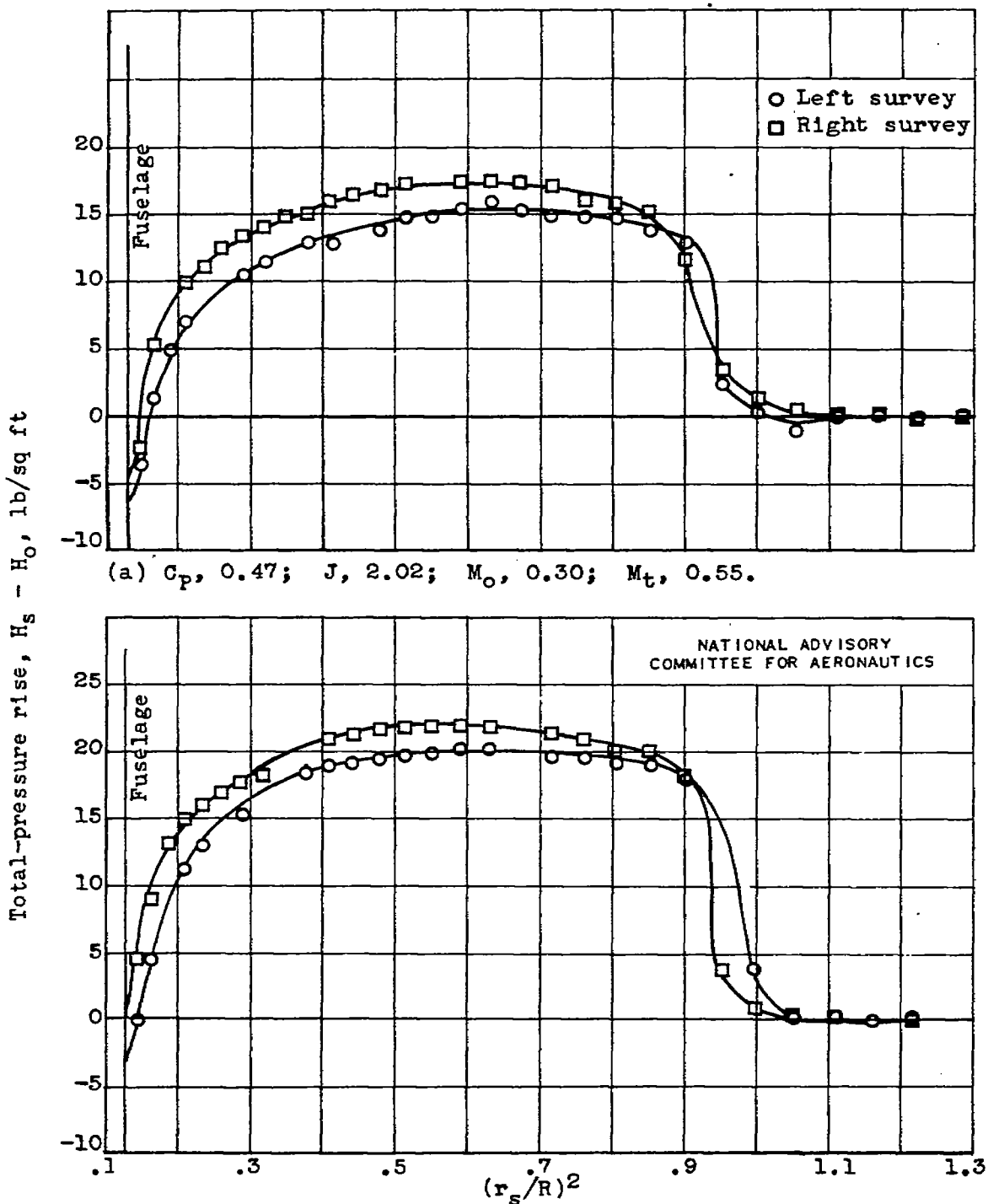

Figure 15.- Effect of advance-diameter ratio J on blade thrust load distribution at power coefficient C_p of approximately 0.50 and free-stream Mach number M_o of approximately 0.30. Hamilton Standard 6507A-2 four-blade propeller.

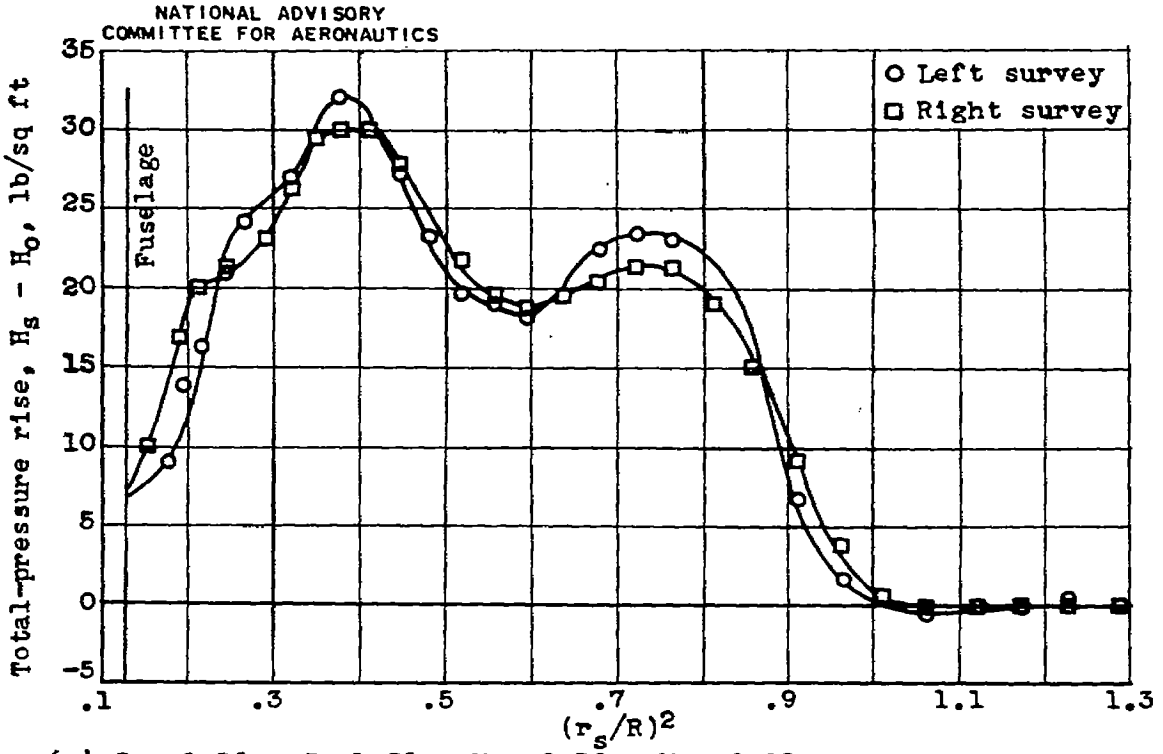

(c) C_p, 0.50; J, 1.21; M_o, 0.30; M_t, 0.82.

Figure 15.- Concluded. Effect of advance-diameter ratio J on blade thrust load distribution at power coefficient C_p of approximately 0.50 and free-stream Mach number M_o of approximately 0.30. Hamilton Standard 6507A-2 four-blade propeller.

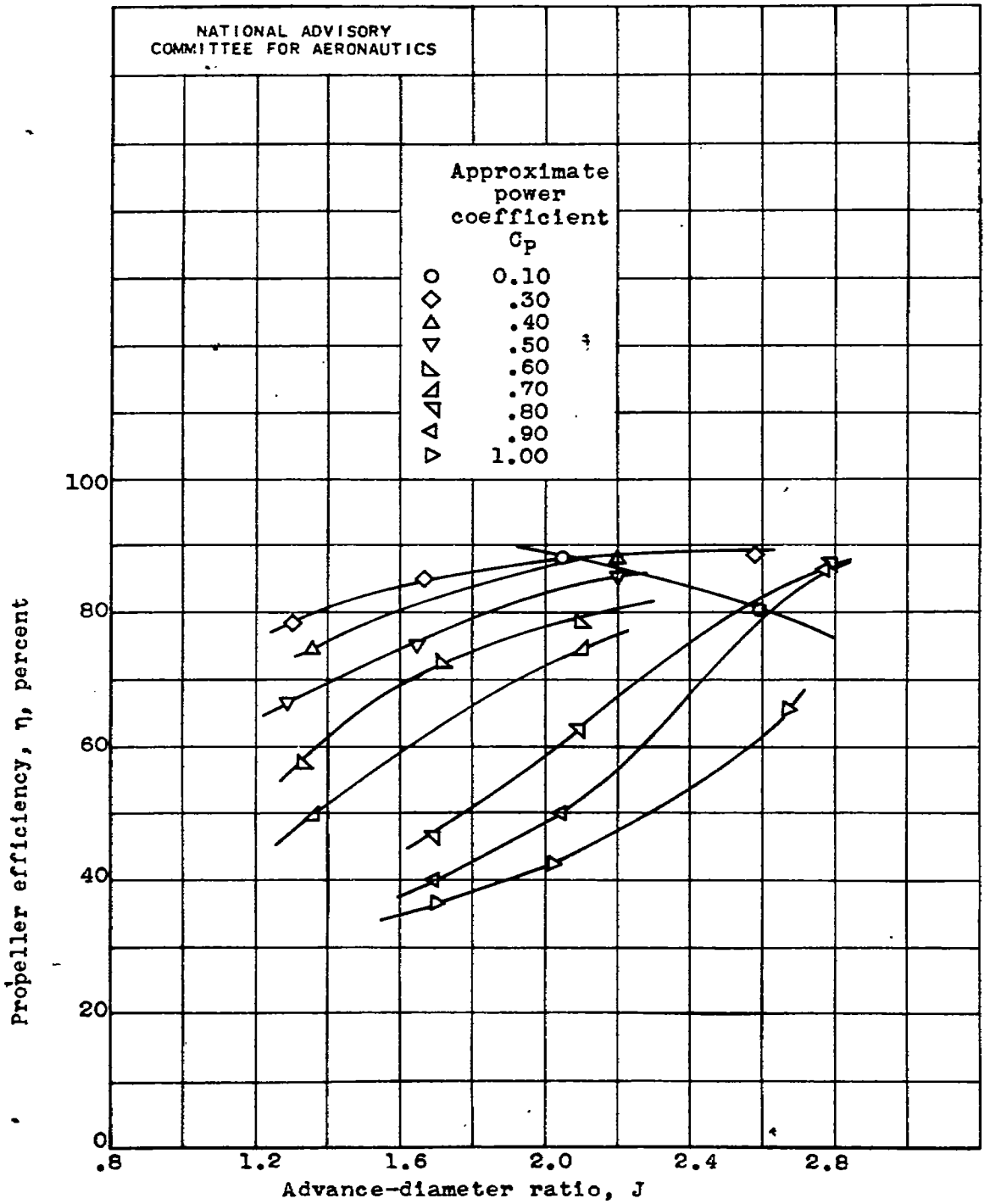

Figure 16.- Characteristics of Hamilton Standard 6507A-2 four-blade propeller on YP-47M airplane at free-stream Mach number M_0 of approximately 0.40.

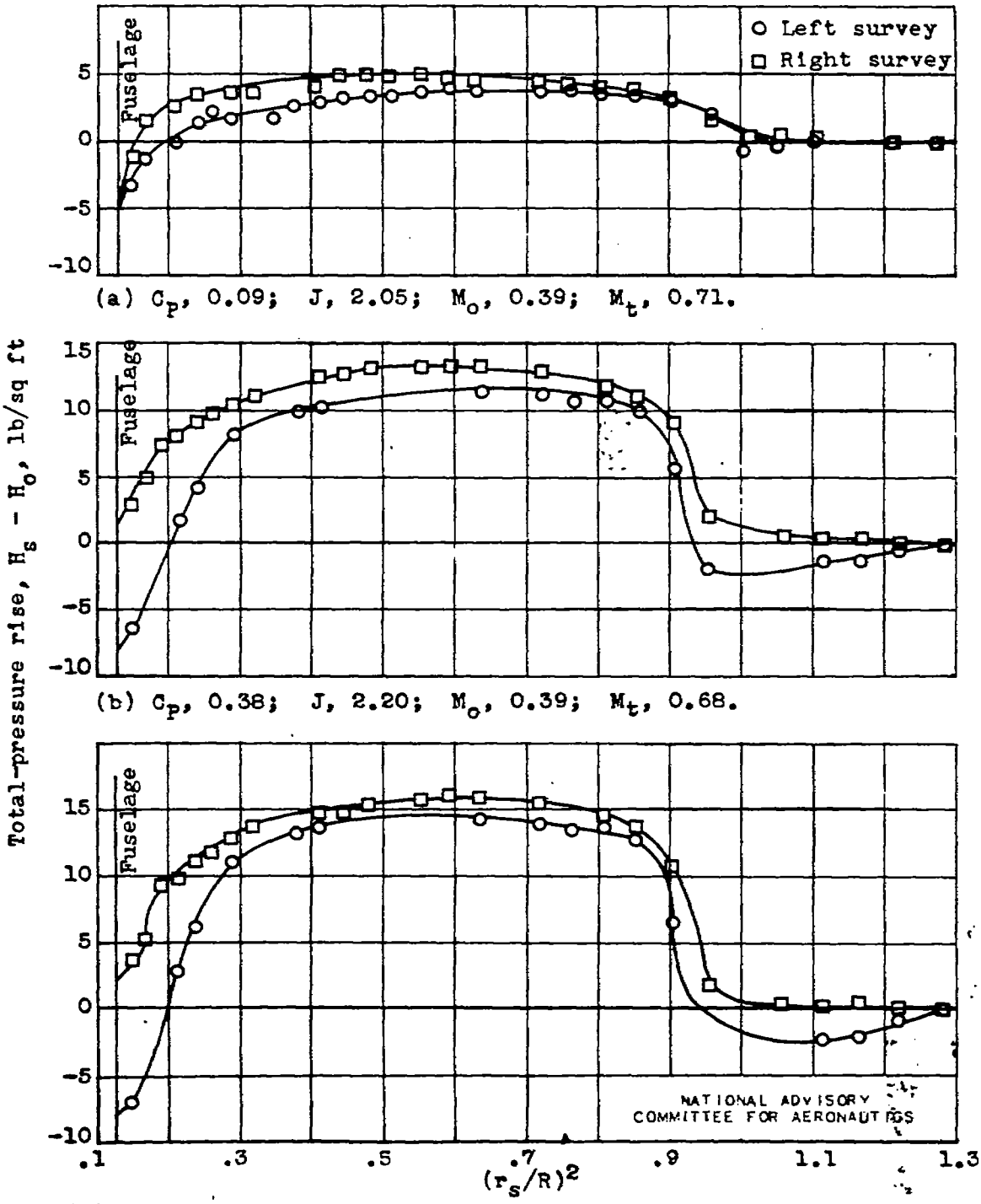

(a) C_p, 0.09; J, 2.05; M_o, 0.39; M_t, 0.71.

(b) C_p, 0.38; J, 2.20; M_o, 0.39; M_t, 0.68.

(c) C_p, 0.48; J, 2.20; M_o, 0.39; M_t, 0.68.

Figure 17.- Effect of power coefficient C_p on blade thrust load distribution at advance-diameter ratio J of approximately 2.10 and free-stream Mach number M_o of approximately 0.40. Hamilton Standard 6507A-2 four-blade propeller.

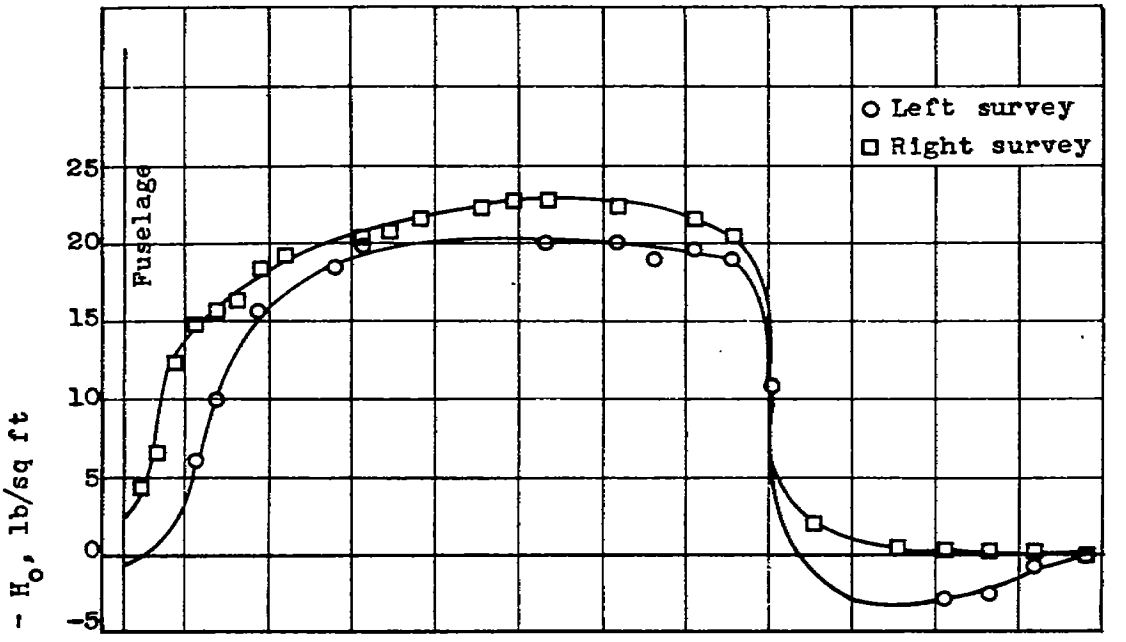

(d) C_p, 0.61; J, 2.15; M_o, 0.40; M_t, 0.71.

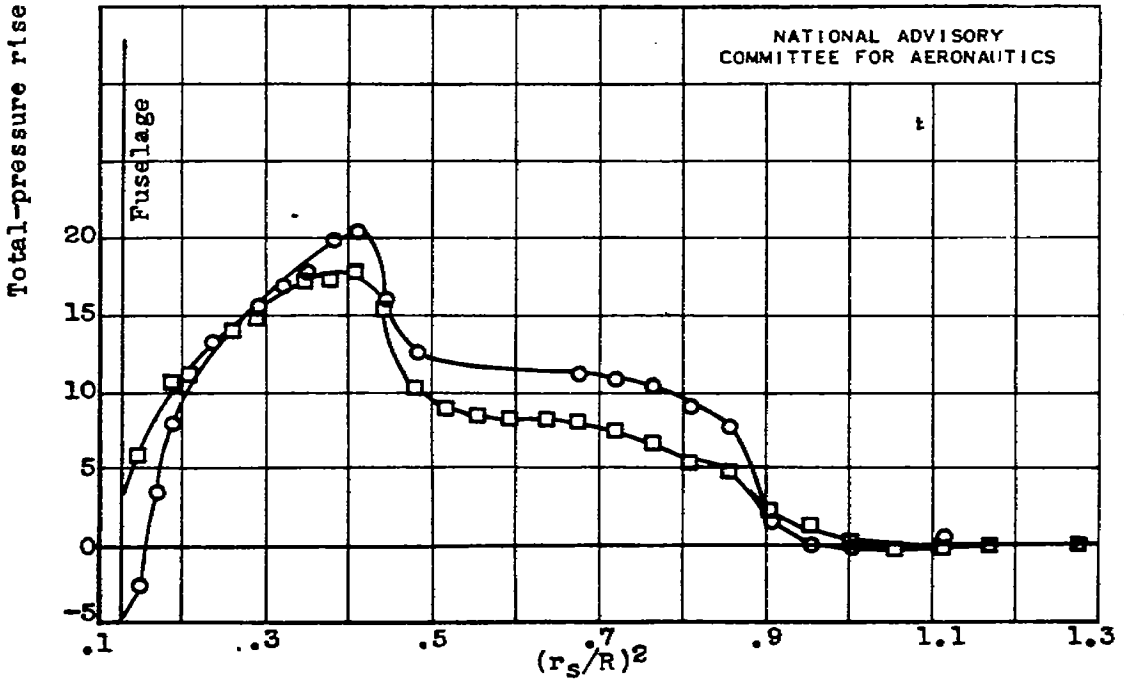

(e) C_p, 0.99; J, 2.03; M_o, 0.38; M_t, 0.70.

Figure 17.- Concluded. Effect of power coefficient C_p on blade thrust load distribution at advance-diameter ratio J of approximately 2.10 and free-stream Mach number M_o of approximately 0.40. Hamilton Standard 6507A-2 four-blade propeller.

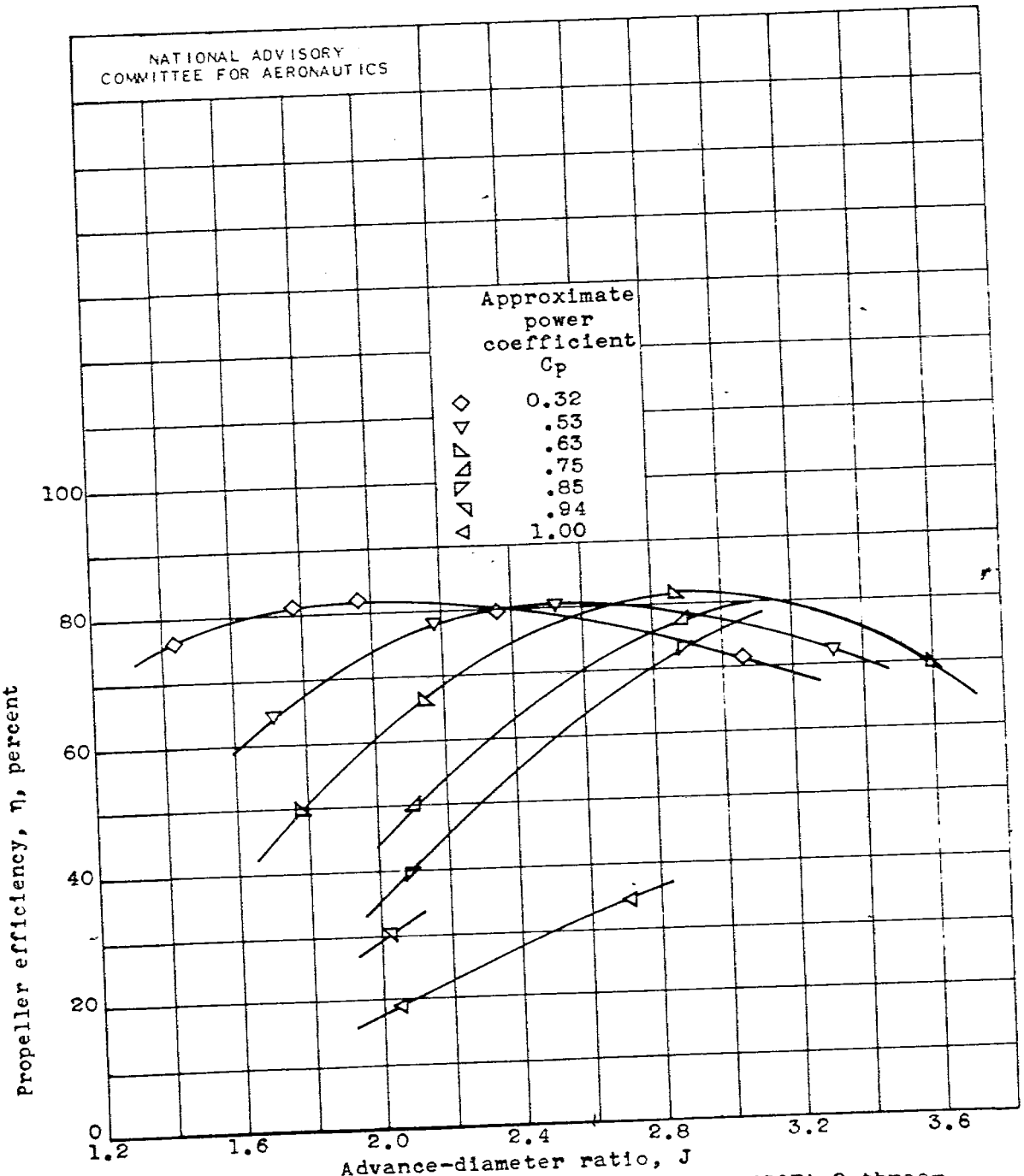

Figure 18.- Characteristics of Hamilton Standard 6507A-2 three-blade propeller on YP-47M airplane at free-stream Mach number M_o of approximately 0.40.

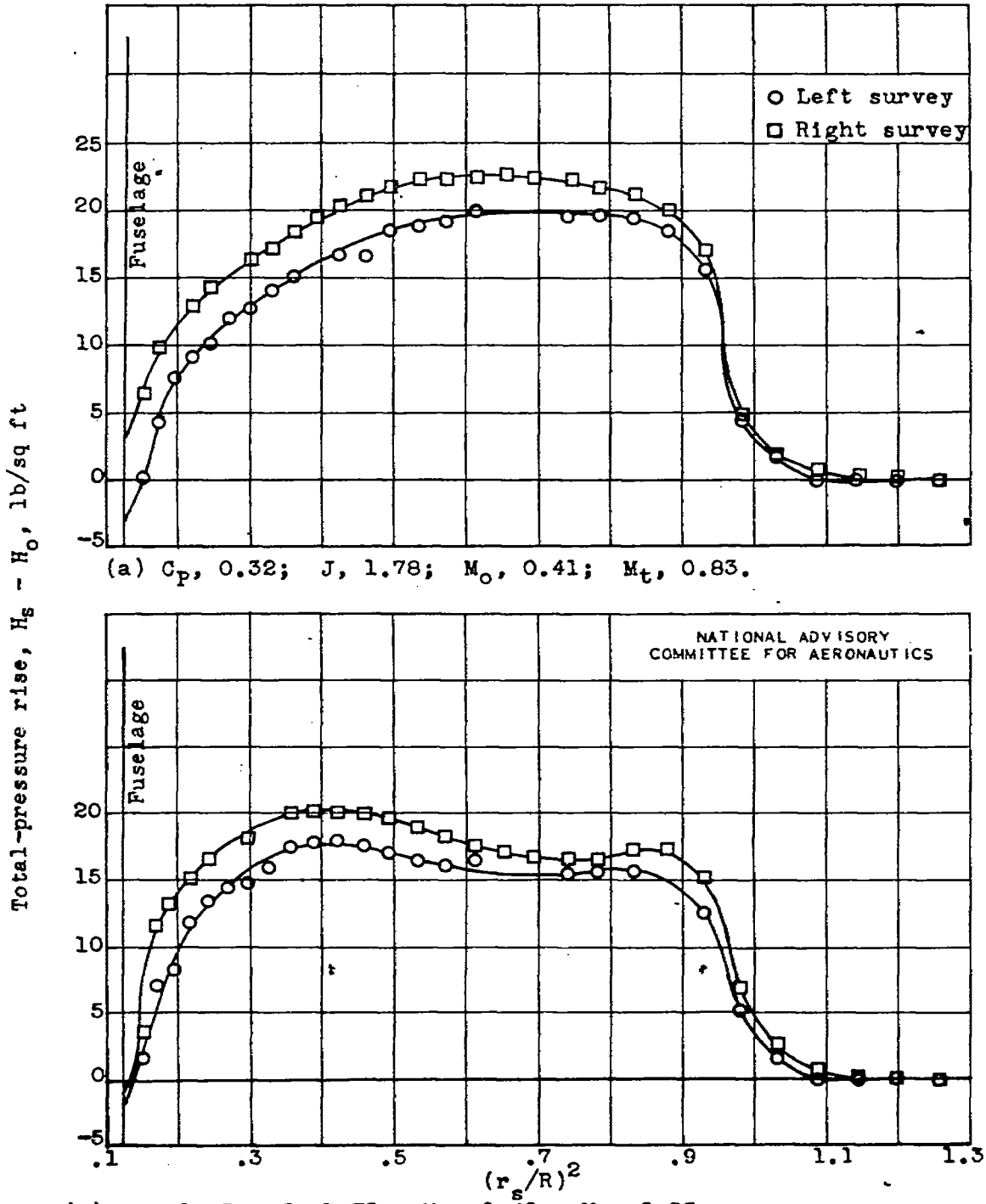

(a) C_p, 0.32; J, 1.78; M_o, 0.41; M_t, 0.83.

(b) C_p, 0.53; J, 1.72; M_o, 0.40; M_t, 0.83.

Figure 19.- Effect of power coefficient C_p on blade thrust load distribution at advance-diameter ratio J of approximately 1.75 and free-stream Mach number M_o of approximately 0.40. Hamilton Standard 6507A-2 three-blade propeller.

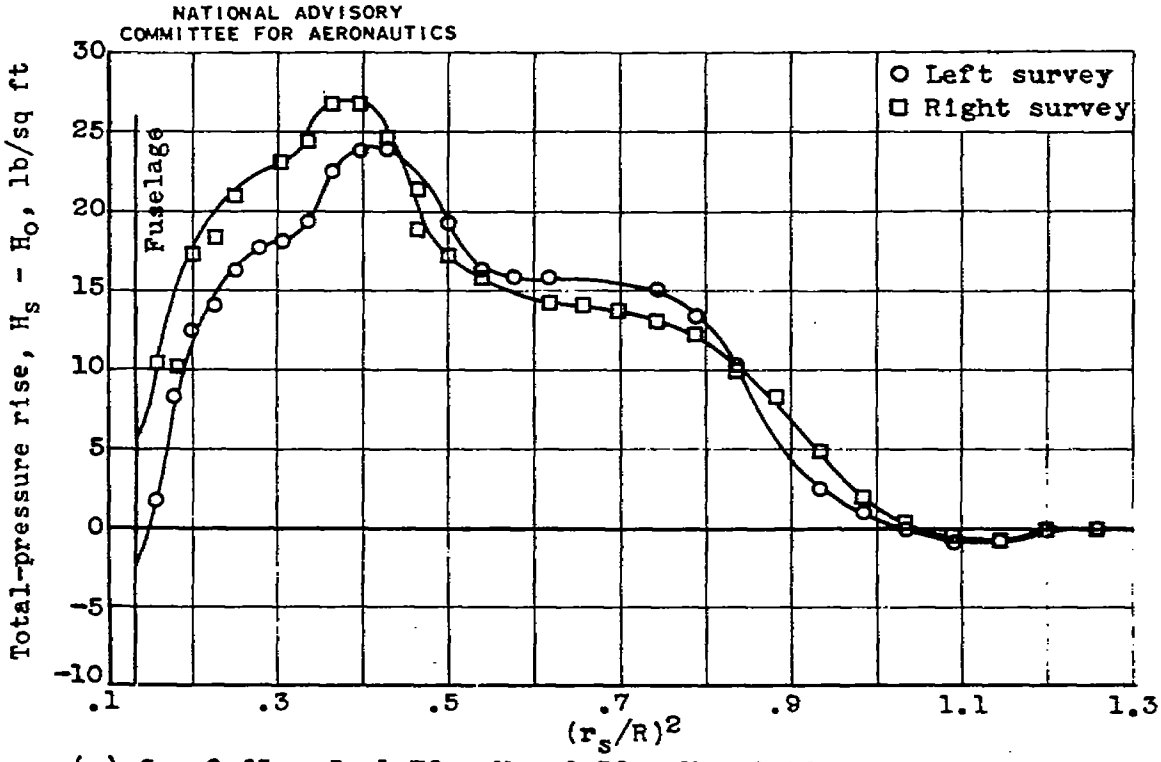

(c) C_p, 0.65; J, 1.78; M_o, 0.39; M_t, 0.80.

Figure 19.- Concluded. Effect of power coefficient C_p on blade thrust load distribution at advance-diameter ratio J of approximately 1.75 and free-stream Mach number M_o of approximately 0.40. Hamilton Standard 6507A-2 three-blade propeller.

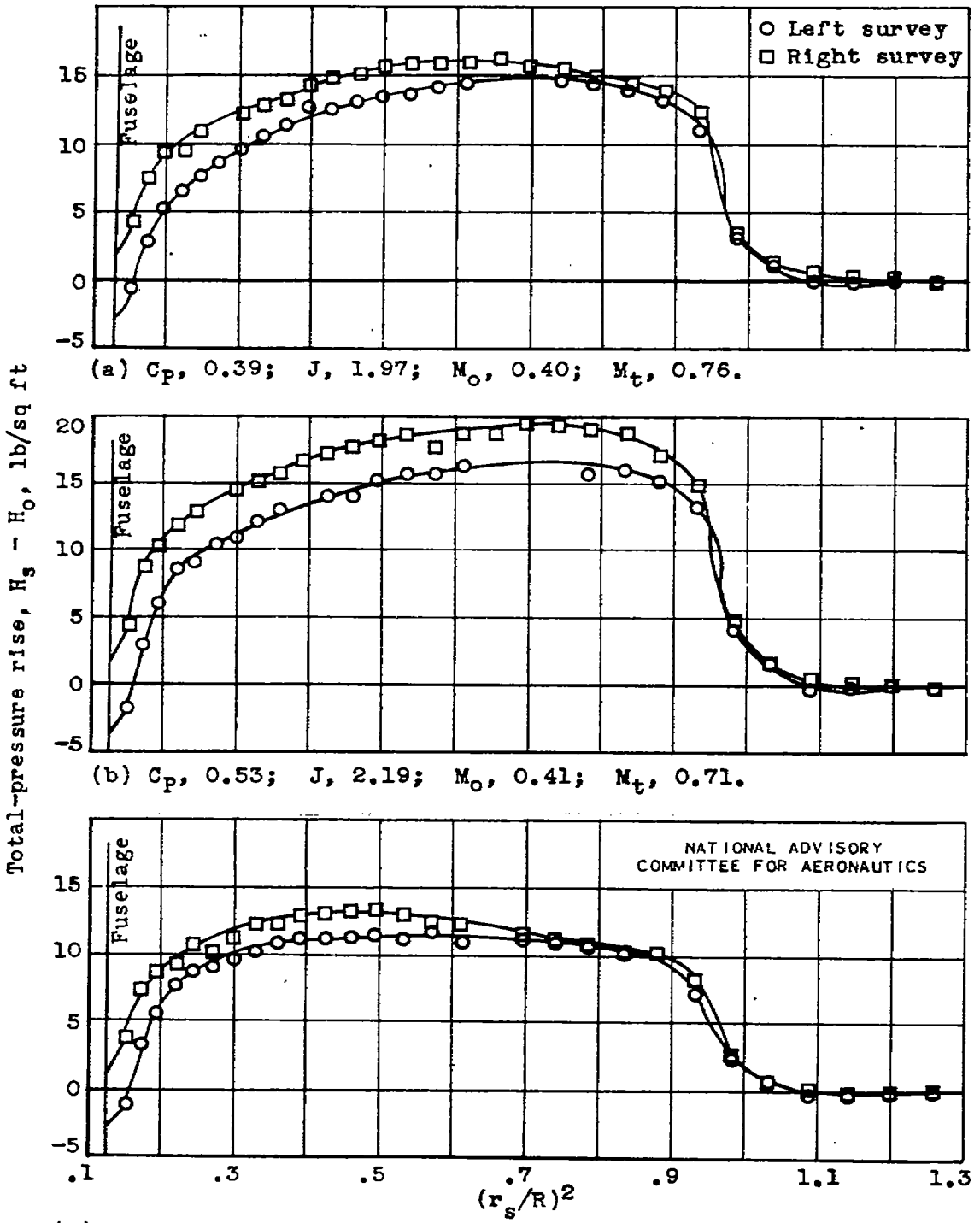

(a) C_p, 0.39; J, 1.97; M_o, 0.40; M_t, 0.76.

(b) C_p, 0.53; J, 2.19; M_o, 0.41; M_t, 0.71.

(c) C_p, 0.63; J, 2.15; M_o, 0.39; M_t, 0.70.

Figure 20.- Effect of power coefficient C_p on blade thrust load distribution at advance-diameter ratio J of approximately 2.10 and free-stream Mach number M_o of approximately 0.40. Hamilton Standard 6507A-2 three-blade propeller.

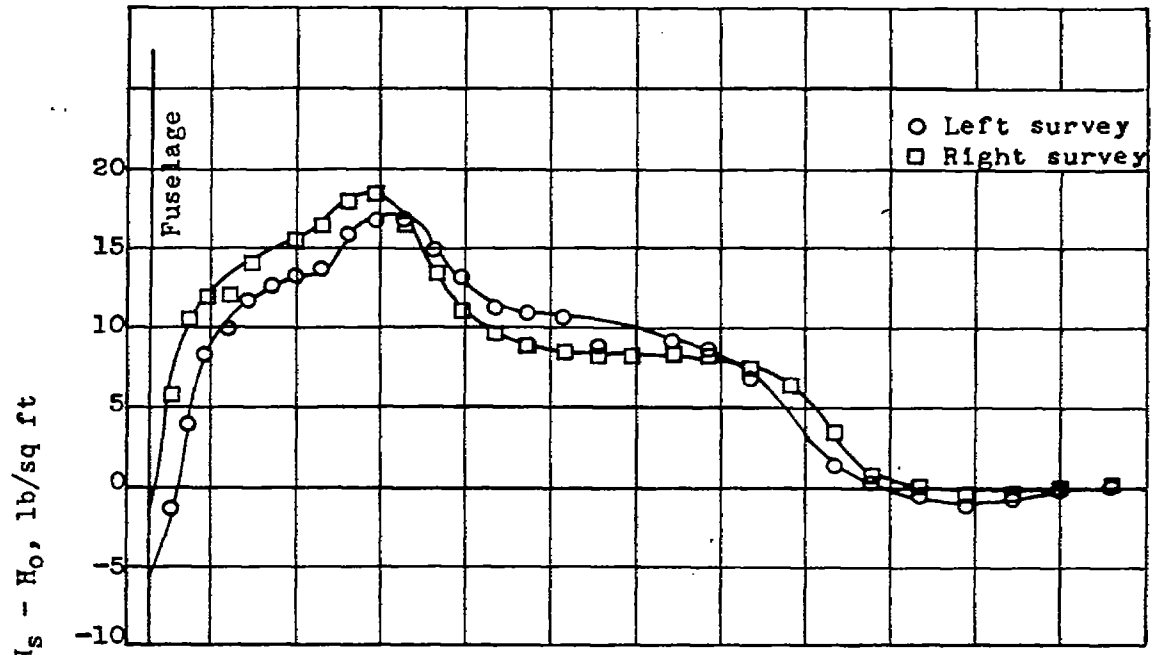

(d) C_p, 0.74; J, 2.11; M_o, 0.39; M_t, 0.69.

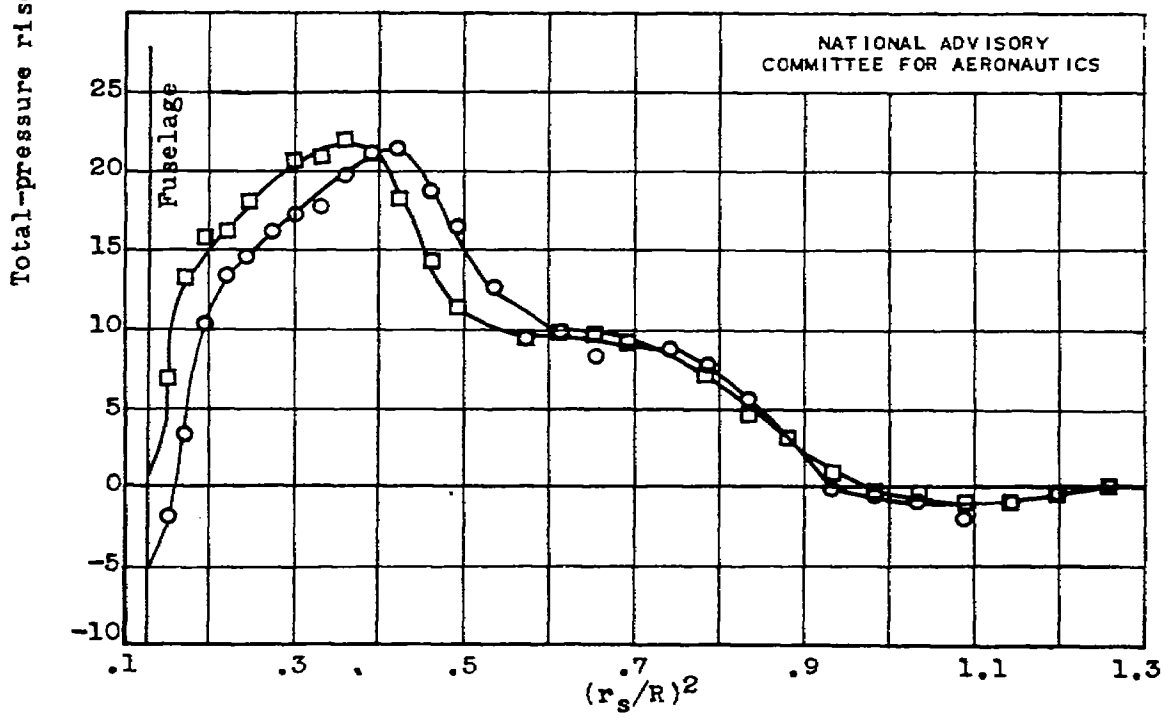

Total-pressure rise, $H_s - H_o$, lb/sq ft

(e) C_p, 0.85; J, 2.09; M_o, 0.38; M_t, 0.69.

Figure 20.- Continued. Effect of power coefficient C_p on blade thrust load distribution at advance-diameter ratio J of approximately 2.10 and free-stream Mach number M_o of approximately 0.40. Hamilton Standard 6507A-2 three-blade propeller.

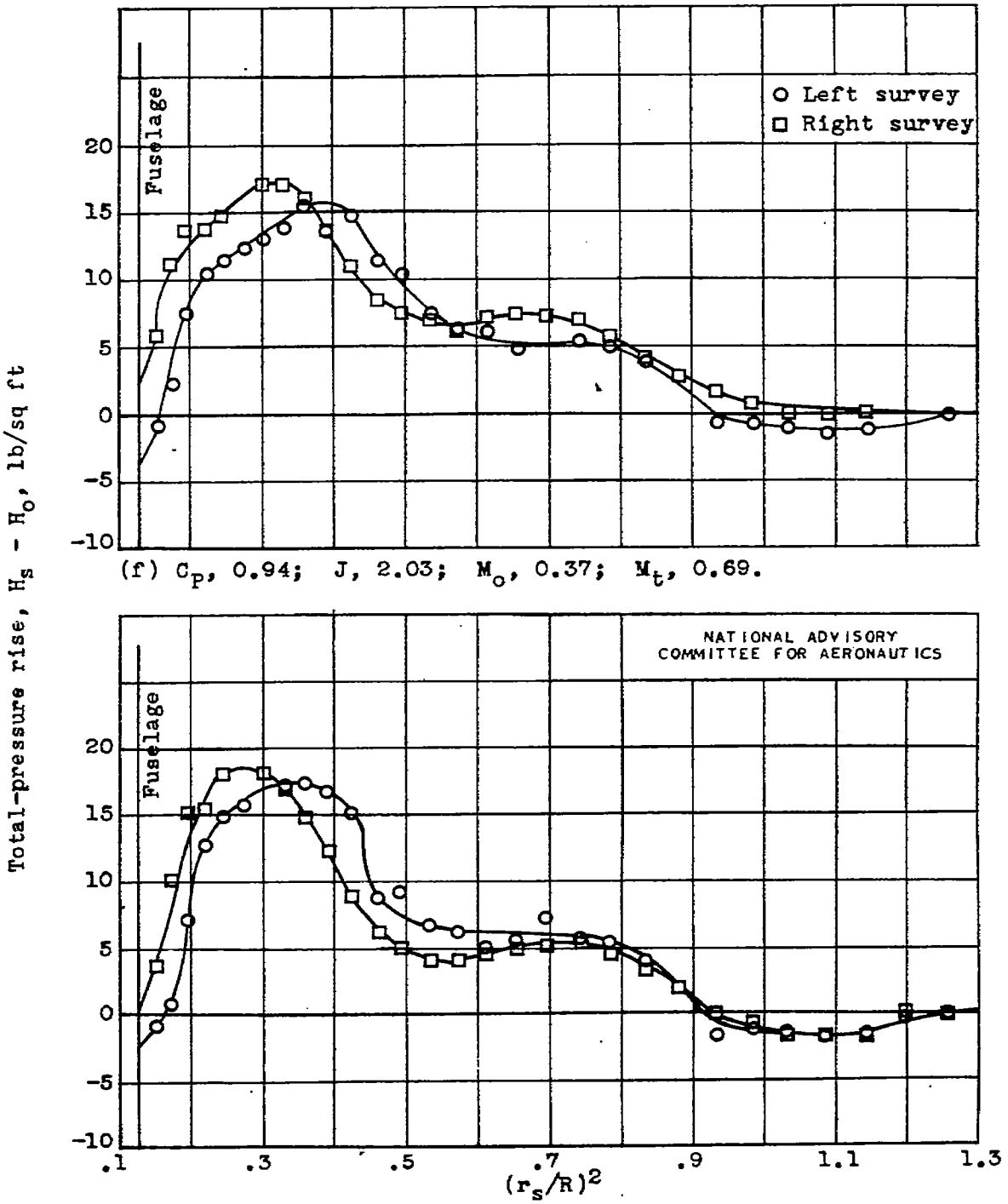

(f) C_p, 0.94; J, 2.03; M_o, 0.37; M_t, 0.69.

(g) C_p, 1.07; J, 2.05; M_o, 0.37; M_t, 0.68.

Figure 20.- Concluded. Effect of power coefficient C_p on blade thrust load distribution at advance-diameter ratio J of approximately 2.10 and free-stream Mach number M_o of approximately 0.40. Hamilton Standard 6507A-2 three-blade propeller.

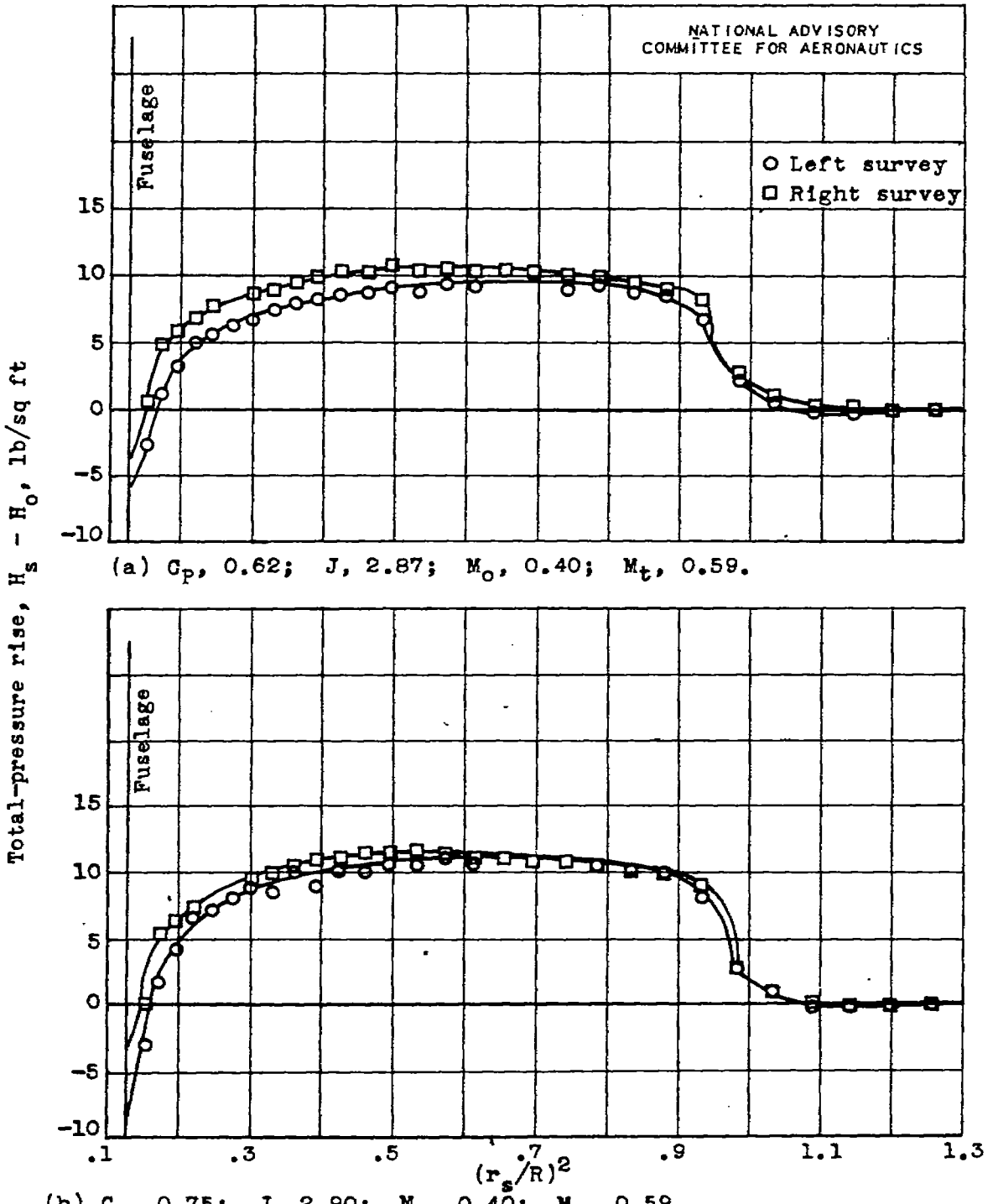

(a) C_p, 0.62; J, 2.87; M_o, 0.40; M_t, 0.59.

(b) C_p, 0.75; J, 2.90; M_o, 0.40; M_t, 0.59.

Figure 21.- Effect of power coefficient C_p on blade thrust load distribution at advance-diameter ratio J of approximately 2.90 and free-stream Mach number M_o of approximately 0.40. Hamilton Standard 6507A-2 three-blade propeller.

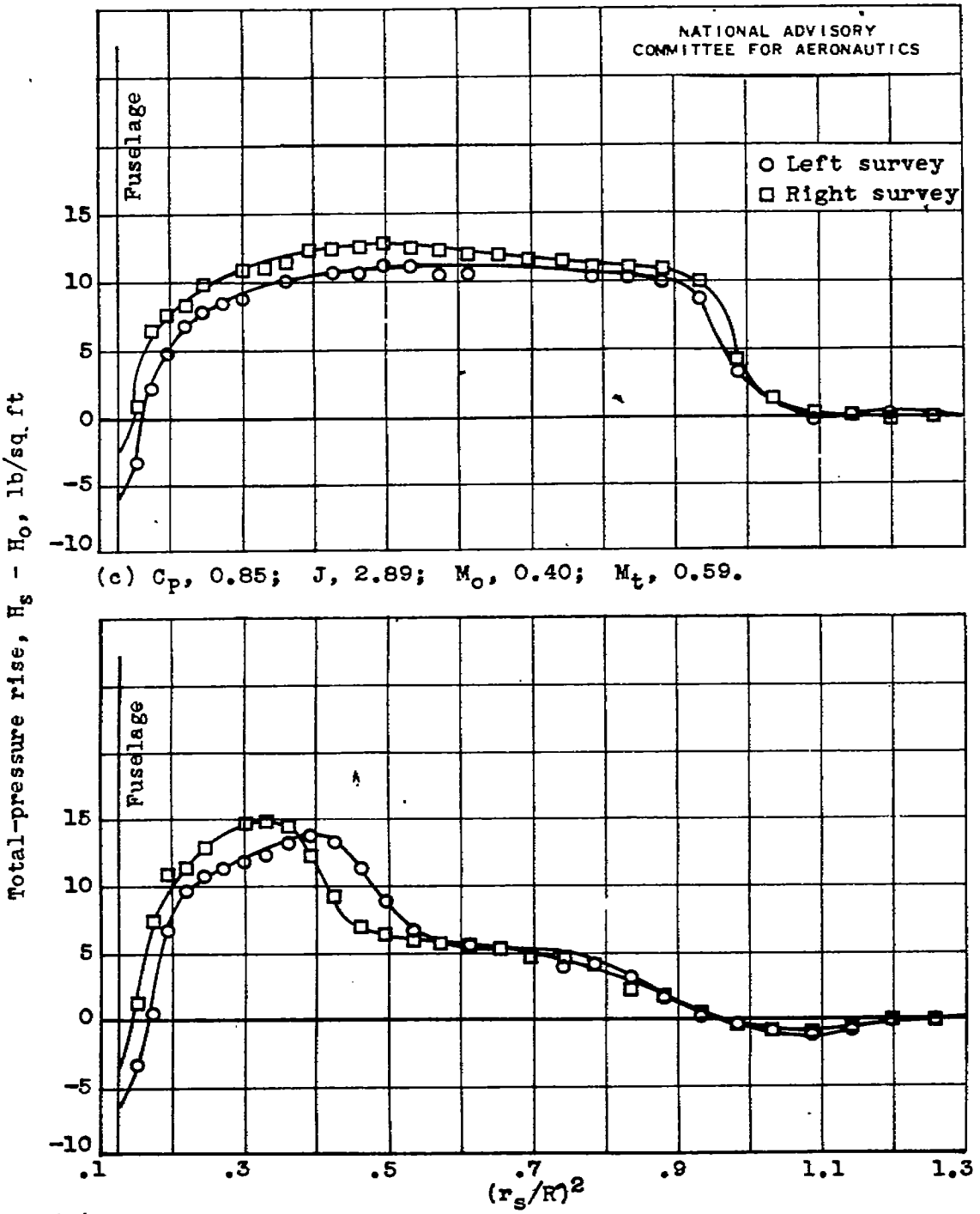

(c) C_p, 0.85; J, 2.89; M_o, 0.40; M_t, 0.59.

(d) C_p, 1.03; J, 2.72; M_o, 0.39; M_t, 0.60.

Figure 21.- Concluded. Effect of power coefficient C_p on blade thrust load distribution at advance-diameter ratio J of approximately 2.90 and free-stream Mach number M_o of approximately 0.40. Hamilton Standard 6507A-2 three-blade propeller.

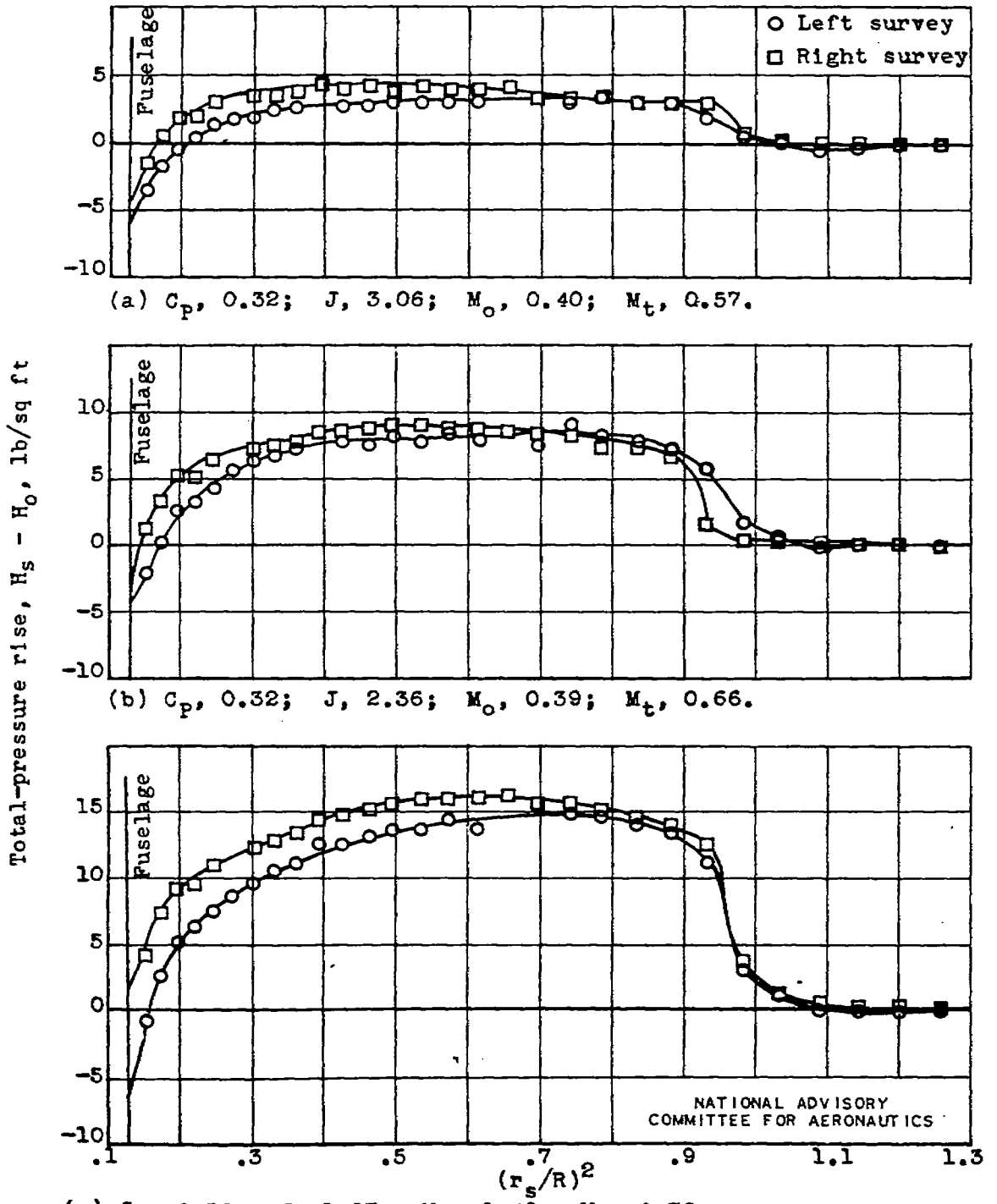

(a) C_p, 0.32; J, 3.06; M_o, 0.40; M_t, 0.57.

(b) C_p, 0.32; J, 2.36; M_o, 0.39; M_t, 0.66.

(c) C_p, 0.32; J, 1.97; M_o, 0.40; M_t, 0.76.

Figure 22.- Effect of advance-diameter ratio J on blade thrust load distribution at power coefficient C_p of approximately 0.32 and free-stream Mach number M_o of approximately 0.40. Hamilton Standard 6507A-2 three-blade propeller.

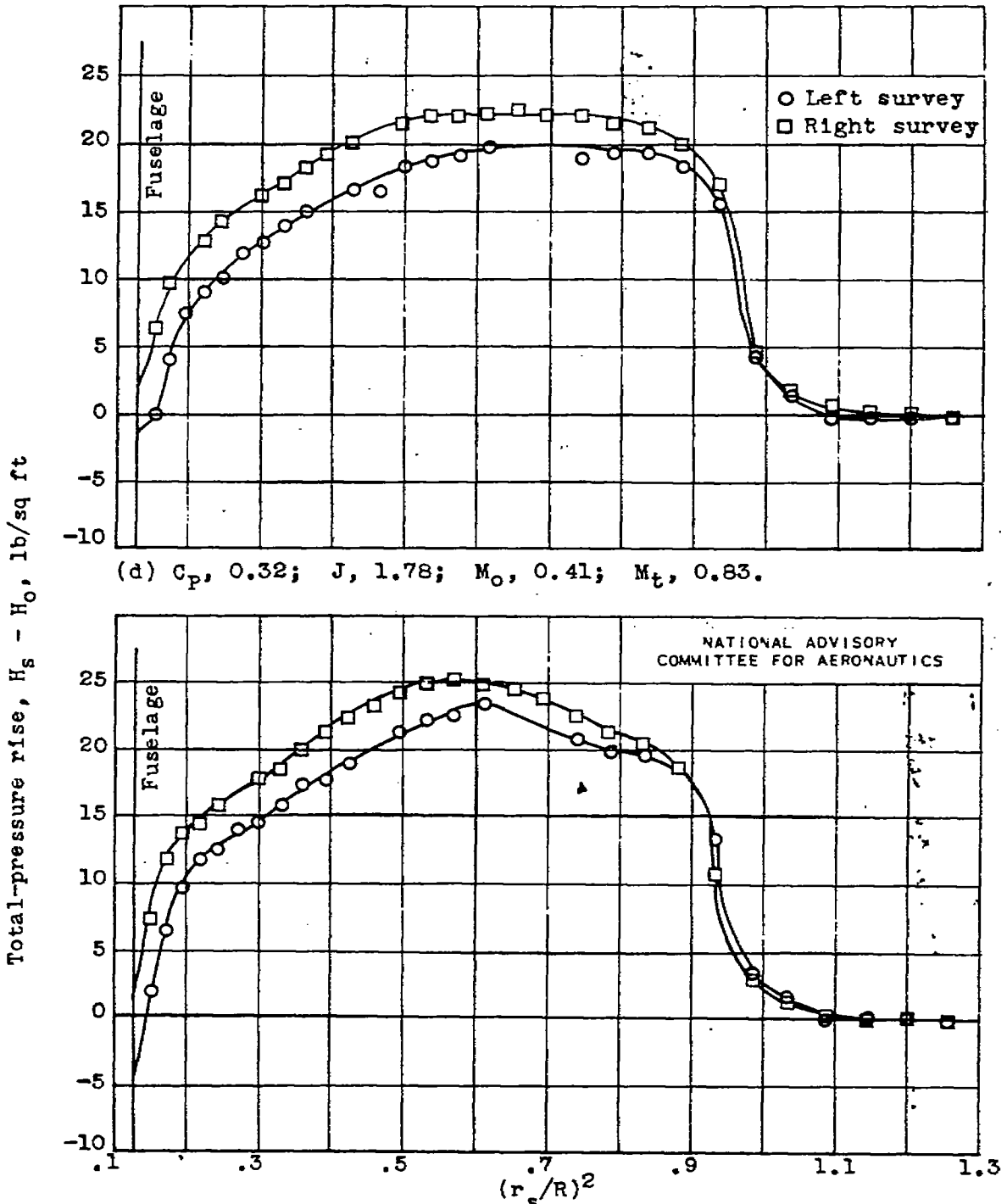

(d) C_p, 0.32; J, 1.78; M_o, 0.41; M_t, 0.83.

(e) C_p, 0.32; J, 1.44; M_o, 0.40; M_t, 0.97.

Figure 22.- Concluded. Effect of advance-diameter ratio J on blade thrust load distribution at power coefficient C_p of approximately 0.32 and free-stream Mach number M_o of approximately 0.40. Hamilton Standard 6507A-2 three-blade propeller.

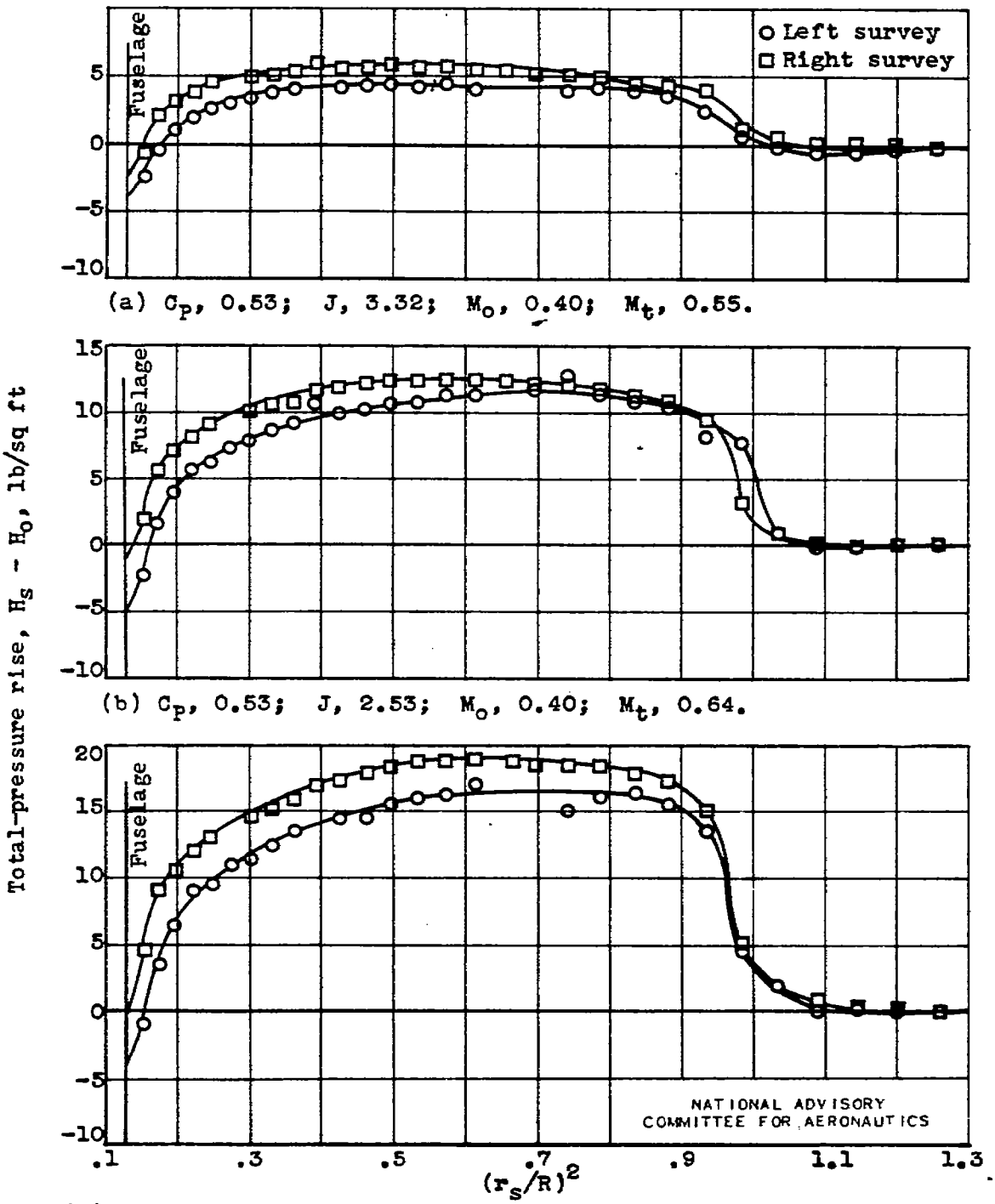

(a) C_p, 0.53; J, 3.32; M_o, 0.40; M_t, 0.55.

(b) C_p, 0.53; J, 2.53; M_o, 0.40; M_t, 0.64.

(c) C_p, 0.53; J, 2.19; M_o, 0.41; M_t, 0.71.

Figure 23.- Effect of advance-diameter ratio J on blade thrust load distribution at power coefficient C_p of approximately 0.53 and free-stream Mach number M_o of approximately 0.40. Hamilton Standard 6507A-2 three-blade propeller.

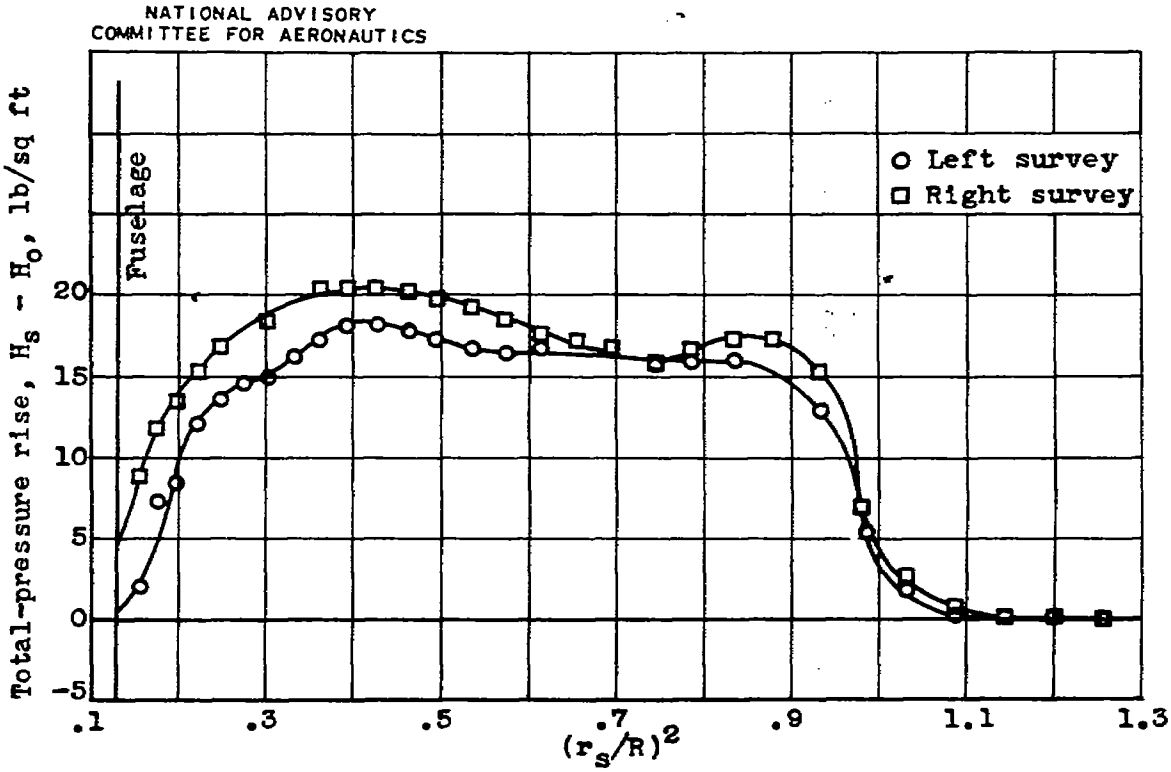

(d) C_p, 0.53; J, 1.72; M_o, 0.40; M_t, 0.83.

Figure 23.- Concluded. Effect of advance-diameter ratio J on blade thrust load distribution at power coefficient C_p of approximately 0.53 and free-stream Mach number M_o of approximately 0.40. Hamilton Standard 6507A-2 three-blade propeller.

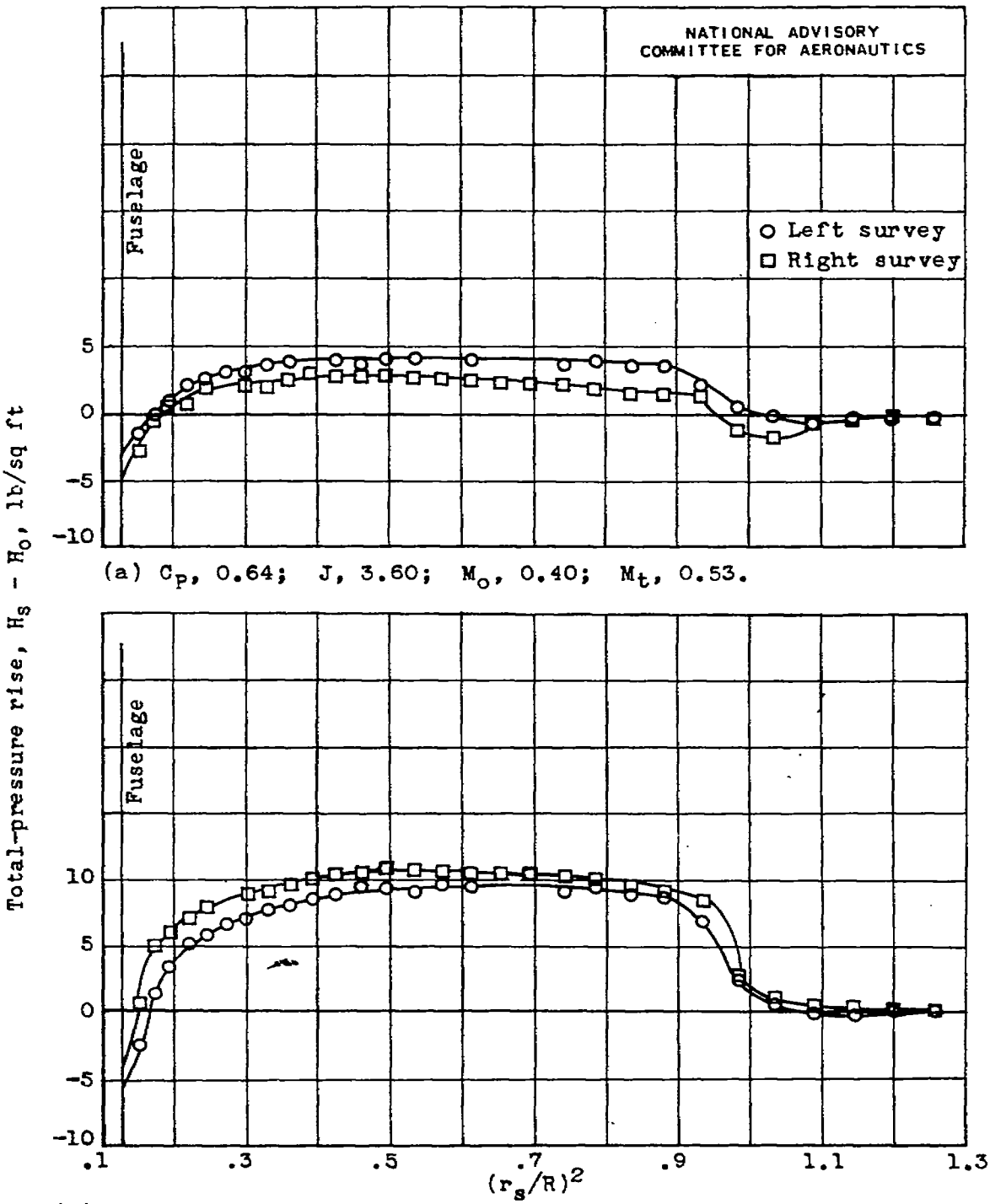

(a) C_p, 0.64; J, 3.60; M_o, 0.40; M_t, 0.53.

(b) C_p, 0.62; J, 2.87; M_o, 0.40; M_t, 0.59.

Figure 24.- Effect of advance-diameter ratio J on blade thrust load distribution at power coefficient C_p of approximately 0.63 and free-stream Mach number M_o of approximately 0.40. Hamilton Standard 6507A-2 three-blade propeller.

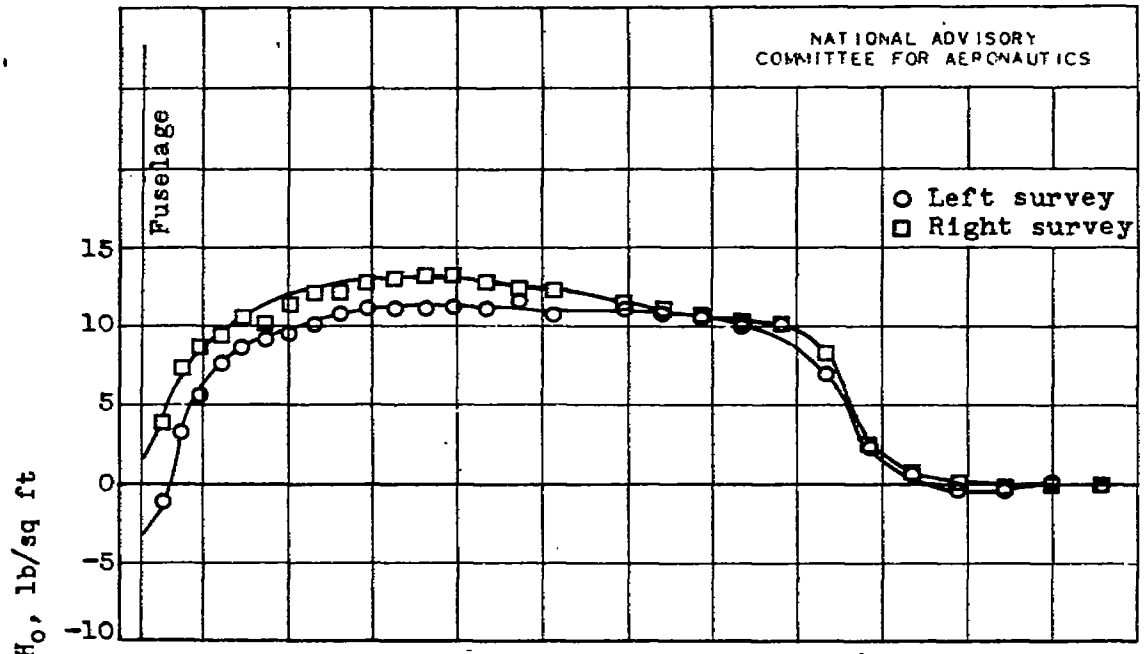

(c) C_p, 0.63; J, 2.15; M_o, 0.39; M_t, 0.70.

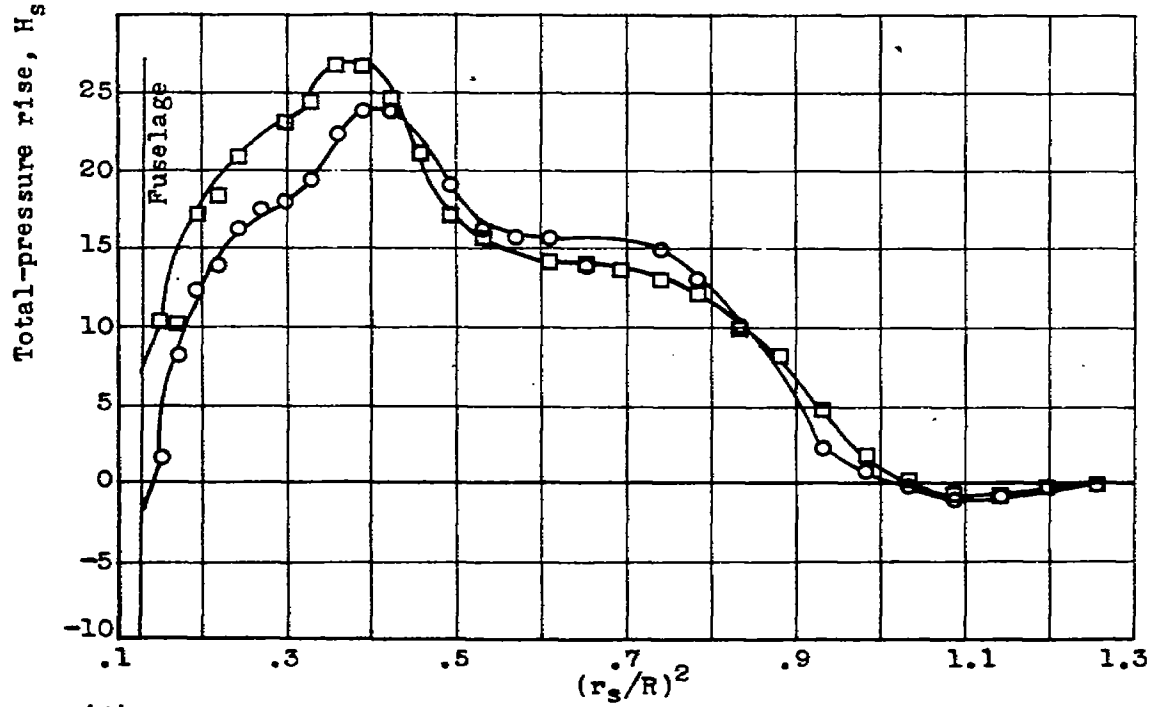

(d) C_p, 0.65; J, 1.78; M_o, 0.39; M_t, 0.80.

Figure 24.- Concluded. Effect of advance-diameter ratio J on blade thrust load distribution at power coefficient C_p of approximately 0.63 and free-stream Mach number M_o of approximately 0.40. Hamilton Standard 6507A-2 three-blade propeller.

(Section 12)

Propellers, Multi-Bladed

11' — Hamilton Standard 6507A-2

Propellers — Reversible

Propellers — Wood

Propellers — High Speed

Airplanes - Curtiss P-47M